## Long-term outcome

The end-point of antiviral therapy is to prevent liver cirrhosis and HCC. Meta-analysis of five studies including 935 patients revealed that IFN treatment significantly decreased the incidence of cirrhosis with the combined risk ratio of 0.65 (95% confidence interval [CI] = 0.47–0.91).[195] Meta-analysis of 11 studies including 2082 patients revealed that IFN treatment significantly decreased the incidence of HCC with the combined risk ratio of 0.59 (95% CI = 0.43–0.81).[195] These results suggest that IFN prevents progression of liver disease to liver cirrhosis or delays the development of HCC, as long as it is within 4–7 years of follow up which is the length of follow up in these studies. Sustained response to IFN therapy was associated with increased survival.[175,181,196,197] To further elucidate the impact of IFN on the natural course of chronic hepatitis B, studies with larger populations followed for longer periods may be needed.

Consensus statement 12

12-1 IFN therapy prevents progression to cirrhosis or the development of HCC. (Level 1a.)

12-2 IFN therapy is associated with improved survival. (Level 1b.)

## Adverse effects

The most frequent adverse effects are flu-like symptoms, fatigue, myelosuppression and dermal reaction at the injection site. Others include alopecia, depression and thyroid dysfunction. Less frequent but severe adverse events include interstitial pneumonitis, exacerbation of underlying autoimmune disorders, cerebral vascular events and flare of hepatitis.

## REFERENCES


1 Lavanchy D. Hepatitis B virus epidemiology, disease burden, treatment, and current and emerging prevention and control measures. *J Viral Hepat* 2004; **11**: 97–107.

2 McMahon BJ, Alward WL, Hall DB *et al.* Acute hepatitis B virus infection: relation of age to the clinical expression of disease and subsequent development of the carrier state. *J Infect Dis* 1985; **151**: 599–603.

3 Shiffman RN, Shenkelle P, Overhage JM, Drimshaw J, Deshpande AM. Standard reporting of clinical practice guidelines: a proposal from the Conference on Guideline Standization. *Ann Intern Med* 2003; **139**: 493–8.

4 McMahon BJ. The natural history of chronic hepatitis B virus infection. *Hepatology* 2009; **49**: S45–55.

5 Fattovich G. Natural history and prognosis of hepatitis B. *Semin Liver Dis* 2003; **23**: 47–58.

6 Chen DS. From hepatitis to hepatoma: lessons from type B viral hepatitis. *Science* 1993; **262**: 369–70.

7 Hoofnagle JH, Doo E, Liang TJ, Fleischer R, Lok AS. Management of hepatitis B: summary of a clinical research workshop. *Hepatology* 2007; **45**: 1056–75.

8 Lok AS. Chronic hepatitis B. *N Engl J Med* 2002; **346**: 1682–3.

9 Lok AS, Heathcote EJ, Hoofnagle JH. Management of hepatitis B: 2000 – summary of a workshop. *Gastroenterology* 2001; **120**: 1828–53.

10 Chang MH, Hsu HY, Hsu HC, Ni YH, Chen JS, Chen DS. The significance of spontaneous hepatitis B e antigen seroconversion in childhood: with special emphasis on the clearance of hepatitis B e antigen before 3 years of age. *Hepatology* 1995; **22**: 1387–92.

11 Hui CK, Leung N, Yuen ST *et al.* Natural history and disease progression in Chinese chronic hepatitis B patients in immune-tolerant phase. *Hepatology* 2007; **46**: 395–401.

12 Lok AS, Lai CL. A longitudinal follow-up of asymptomatic hepatitis B surface antigen-positive Chinese children. *Hepatology* 1988; **8**: 1130–3.

13 Bortolotti F, Guido M, Bartolacci S *et al.* Chronic hepatitis B in children after e antigen seroclearance: final report of a 29-year longitudinal study. *Hepatology* 2006; **43**: 556–62.

14 Chu CM, Hung SJ, Lin J, Tai DI, Liaw YF Natural history of hepatitis B e antigen to antibody seroconversion in patients with normal serum aminotransferase levels. *Am J Med* 2004; **116**: 829–34.

15 Hoofnagle JH, Dusheiko GM, Seeff LB, Jones EA, Waggoner JG, Bales ZB. Seroconversion from hepatitis B e antigen to antibody in chronic type B hepatitis. *Ann Intern Med* 1981; **94**: 744–8.

16 McMahon BJ. Epidemiology and natural history of hepatitis B. *Semin Liver Dis* 2005; **25** (Suppl 1): 3–8.

17 Fattovich G, Rugge M, Brollo L *et al.* Clinical, virologic and histologic outcome following seroconversion from HBeAg to anti-HBe in chronic hepatitis type B. *Hepatology* 1986; **6**: 167–72.

18 Liaw YF, Chu CM, Huang MJ, Sheen IS, Yang CY, Lin DY. Determinants for hepatitis B e antigen clearance in chronic type B hepatitis. *Liver* 1984; **4**: 301–6.

19 Lok AS, Lai CL, Wu PC, Leung EK, Lam TS. Spontaneous hepatitis B e antigen to antibody seroconversion and reversion in Chinese patients with chronic hepatitis B virus infection. *Gastroenterology* 1987; **92**: 1839–43.

20 McMahon BJ, Holck P, Bulkow L, Snowball M. Serologic and clinical outcomes of 1536 Alaska Natives chronically infected with hepatitis B virus. *Ann Intern Med* 2001; **135**: 759–68.

21 Yuen MF, Yuan HJ, Hui CK *et al.* A large population study of spontaneous HBeAg seroconversion and acute exacer-

bation of chronic hepatitis B infection: implications for antiviral therapy. *Gut* 2003; **52**: 416–19.
22 Kao JH, Chen PJ, Lai MY, Chen DS. Hepatitis B genotypes correlate with clinical outcomes in patients with chronic hepatitis B. *Gastroenterology* 2000; **118**: 554–9.
23 Chu CJ, Hussain M, Lok AS. Hepatitis B virus genotype B is associated with earlier HBeAg seroconversion compared with hepatitis B virus genotype C. *Gastroenterology* 2002; **122**: 1756–62.
24 Hsu YS, Chien RN, Yeh CT *et al.* Long-term outcome after spontaneous HBeAg seroconversion in patients with chronic hepatitis B. *Hepatology* 2002; **35**: 1522–7.
25 Carman WF, Jacyna MR, Hadziyannis S *et al.* Mutation preventing formation of hepatitis B e antigen in patients with chronic hepatitis B infection. *Lancet* 1989; **2**: 588–91.
26 Chan HL, Hussain M, Lok AS. Different hepatitis B virus genotypes are associated with different mutations in the core promoter and precore regions during hepatitis B e antigen seroconversion. *Hepatology* 1999; **29**: 976–84.
27 Chen CH, Hung CH, Lee CM *et al.* Pre-S deletion and complex mutations of hepatitis B virus related to advanced liver disease in HBeAg-negative patients. *Gastroenterology* 2007; **133**: 1466–74.
28 Marschenz S, Endres AS, Brinckmann A *et al.* Functional analysis of complex hepatitis B virus variants associated with development of liver cirrhosis. *Gastroenterology* 2006; **131**: 765–80.
29 Chen CH, Changchien CS, Lee CM *et al.* Combined mutations in pre-s/surface and core promoter/precore regions of hepatitis B virus increase the risk of hepatocellular carcinoma: a case–control study. *J Infect Dis* 2008; **198**: 1634–42.
30 Yuen MF, Tanaka Y, Shinkai N *et al.* Risk for hepatocellular carcinoma with respect to hepatitis B virus genotypes B/C, specific mutations of enhancer II/core promoter/precore regions and HBV DNA levels. *Gut* 2008; **57**: 98–102.
31 Ikeda K, Saitoh S, Koida I *et al.* A multivariate analysis of risk factors for hepatocellular carcinogenesis: a prospective observation of 795 patients with viral and alcoholic cirrhosis. *Hepatology* 1993; **18**: 47–53.
32 Yu MW, Chang HC, Liaw YF *et al.* Familial risk of hepatocellular carcinoma among chronic hepatitis B carriers and their relatives. *J Natl Cancer Inst* 2000; **92**: 1159–64.
33 Chen CJ, Yang HI, Su J *et al.* Risk of hepatocellular carcinoma across a biological gradient of serum hepatitis B virus DNA level. *JAMA* 2006; **295**: 65–73.
34 Ishiguro S, Inoue M, Tanaka Y, Mizokami M, Iwasaki M, Tsugane S. Serum aminotransferase level and the risk of hepatocellular carcinoma: a population-based cohort study in Japan. *Eur J Cancer Prev* 2009; **18**: 26–32.
35 Kao JH, Chen PJ, Lai MY, Chen DS. Basal core promoter mutations of hepatitis B virus increase the risk of hepatocellular carcinoma in hepatitis B carriers. *Gastroenterology* 2003; **124**: 327–34.
36 Yu MW, Yeh SH, Chen PJ *et al.* Hepatitis B virus genotype and DNA level and hepatocellular carcinoma: a prospective study in men. *J Natl Cancer Inst* 2005; **97**: 265–72.
37 Benvegnu L, Gios M, Boccato S, Alberti A. Natural history of compensated viral cirrhosis: a prospective study on the incidence and hierarchy of major complications. *Gut* 2004; **53**: 744–9.
38 Ohnishi K, Iida S, Iwama S *et al.* The effect of chronic habitual alcohol intake on the development of liver cirrhosis and hepatocellular carcinoma: relation to hepatitis B surface antigen carriage. *Cancer* 1982; **49**: 672–7.
39 Yu MC, Yuan JM. Environmental factors and risk for hepatocellular carcinoma. *Gastroenterology* 2004; **127**: S72–78.
40 Manno M, Camma C, Schepis F *et al.* Natural history of chronic HBV carriers in northern Italy: morbidity and mortality after 30 years. *Gastroenterology* 2004; **127**: 756–63.
41 Chen YC, Sheen IS, Chu CM, Liaw YF. Prognosis following spontaneous HBsAg seroclearance in chronic hepatitis B patients with or without concurrent infection. *Gastroenterology* 2002; **123**: 1084–9.
42 Huo TI, Wu JC, Lee PC *et al.* Sero-clearance of hepatitis B surface antigen in chronic carriers does not necessarily imply a good prognosis. *Hepatology* 1998; **28**: 231–6.
43 Hui CK, Cheung WW, Zhang HY *et al.* Kinetics and risk of de novo hepatitis B infection in HBsAg-negative patients undergoing cytotoxic chemotherapy. *Gastroenterology* 2006; **131**: 59–68.
44 Tanaka E, Umemura T. History and prevention of de novo hepatitis B virus-related hepatitis in Japan and the World. *Clin J Gastroenterol* 2008; **1**: 83–6.
45 Umemura T, Kiyosawa K. Fatal HBV reactivation in a subject with anti-HBs and anti-HBc. *Intern Med* 2006; **45**: 747–8.
46 Umemura T, Tanaka E, Kiyosawa K, Kumada H. Mortality secondary to fulminant hepatic failure in patients with prior resolution of hepatitis B virus infection in Japan. *Clin Infect Dis* 2008; **47**: e52–56.
47 Taylor BC, Yuan JM, Shamliyan TA, Shaukat A, Kane RL, Wilt TJ. Clinical outcomes in adults with chronic hepatitis B in association with patient and viral characteristics: a systematic review of evidence. *Hepatology* 2009; **49**: S85–95.
48 Kurbanov F, Tanaka Y, Mizokami M. Geographical and genetic diversity of the human hepatitis B virus. *Hepatol Res* 2010; **40**: 14–30.
49 Chen DS. Hepatitis B vaccination: the key towards elimination and eradication of hepatitis B. *J Hepatol* 2009; **50**: 805–16.
50 Lok AS. Natural history and control of perinatally acquired hepatitis B virus infection. *Dig Dis* 1992; **10**: 46–52.
51 Koibuchi T, Hitani A, Nakamura T *et al.* Predominance of genotype A HBV in an HBV-HIV-1 dually positive

population compared with an HIV-1-negative counterpart in Japan. *J Med Virol* 2001; **64**: 435–40.
52 Shibayama T, Masuda G, Ajisawa A *et al.* Characterization of seven genotypes (A to E, G and H) of hepatitis B virus recovered from Japanese patients infected with human immunodeficiency virus type 1. *J Med Virol* 2005; **76**: 24–32.
53 Kobayashi M, Arase Y, Ikeda K *et al.* Viral genotypes and response to interferon in patients with acute prolonged hepatitis B virus infection of adulthood in Japan. *J Med Virol* 2002; **68**: 522–8.
54 Ozasa A, Tanaka Y, Orito E *et al.* Influence of genotypes and precore mutations on fulminant or chronic outcome of acute hepatitis B virus infection. *Hepatology* 2006; **44**: 326–34.
55 Sugauchi F, Orito E, Ohno T *et al.* Spatial and chronological differences in hepatitis B virus genotypes from patients with acute hepatitis B in Japan. *Hepatol Res* 2006; **36**: 107–14.
56 Suzuki Y, Kobayashi M, Ikeda K *et al.* Persistence of acute infection with hepatitis B virus genotype A and treatment in Japan. *J Med Virol* 2005; **76**: 33–9.
57 Matsuura K, Tanaka Y, Hige S *et al.* Distribution of hepatitis B virus genotypes among patients with chronic infection in Japan shifting toward an increase of genotype A. *J Clin Microbiol* 2009; **47**: 1476–83.
58 Sherlock S. The natural history of hepatitis B. *Postgrad Med J* 1987; **63** (Suppl 2): 7–11.
59 Sugiyama M, Tanaka Y, Kato T *et al.* Influence of hepatitis B virus genotypes on the intra- and extracellular expression of viral DNA and antigens. *Hepatology* 2006; **44**: 915–24.
60 Sugiyama M, Tanaka Y, Kurbanov F *et al.* Direct cytopathic effects of particular hepatitis B virus genotypes in severe combined immunodeficiency transgenic with urokinase-type plasminogen activator mouse with human hepatocytes. *Gastroenterology* 2009; **136**: 652–62. e3.
61 Fujiwara K, Mochida S, Matsui A, Nakayama N, Nagoshi S, Toda G. Fulminant hepatitis and late onset hepatic failure in Japan. *Hepatol Res* 2008; **38**: 646–57.
62 Sato S, Suzuki K, Akahane Y *et al.* Hepatitis B virus strains with mutations in the core promoter in patients with fulminant hepatitis. *Ann Intern Med* 1995; **122**: 241–8.
63 Omata M, Ehata T, Yokosuka O, Hosoda K, Ohto M. Mutations in the precore region of hepatitis B virus DNA in patients with fulminant and severe hepatitis. *N Engl J Med* 1991; **324**: 1699–704.
64 Liang TJ, Hasegawa K, Rimon N, Wands JR, Ben-Porath E. A hepatitis B virus mutant associated with an epidemic of fulminant hepatitis. *N Engl J Med* 1991; **324**: 1705–9.
65 Laskus T, Persing DH, Nowicki MJ, Mosley JW, Rakela J. Nucleotide sequence analysis of the precore region in patients with fulminant hepatitis B in the United States. *Gastroenterology* 1993; **105**: 1173–8.
66 Feray C, Gigou M, Samuel D, Bernuau J, Bismuth H, Brechot C. Low prevalence of precore mutations in hepatitis B virus DNA in fulminant hepatitis type B in France. *J Hepatol* 1993; **18**: 119–22.
67 Liang TJ, Hasegawa K, Munoz SJ *et al.* Hepatitis B virus precore mutation and fulminant hepatitis in the United States. A polymerase chain reaction-based assay for the detection of specific mutation. *J Clin Invest* 1994; **93**: 550–5.
68 Chan HL, Sung JJ. Hepatocellular carcinoma and hepatitis B virus. *Semin Liver Dis* 2006; **26**: 153–61.
69 Lok AS. Hepatitis B: liver fibrosis and hepatocellular carcinoma. *Gastroenterol Clin Biol* 2009; **33**: 911–15.
70 Lok AS, McMahon BJ. Chronic hepatitis B. *Hepatology* 2007; **45**: 507–39.
71 Chan HL, Tse CH, Mo F *et al.* High viral load and hepatitis B virus subgenotype ce are associated with increased risk of hepatocellular carcinoma. *J Clin Oncol* 2008; **26**: 177–82.
72 Chen G, Lin W, Shen F, Iloeje UH, London WT, Evans AA. Past HBV viral load as predictor of mortality and morbidity from HCC and chronic liver disease in a prospective study. *Am J Gastroenterol* 2006; **101**: 1797–803.
73 Chan HL, Hui AY, Wong ML *et al.* Genotype C hepatitis B virus infection is associated with an increased risk of hepatocellular carcinoma. *Gut* 2004; **53**: 1494–8.
74 Sumi H, Yokosuka O, Seki N *et al.* Influence of hepatitis B virus genotypes on the progression of chronic type B liver disease. *Hepatology* 2003; **37**: 19–26.
75 Tanaka Y, Mukaide M, Orito E *et al.* Specific mutations in enhancer II/core promoter of hepatitis B virus subgenotypes C1/C2 increase the risk of hepatocellular carcinoma. *J Hepatol* 2006; **45**: 646–53.
76 Huang Y, Wang Z, An S *et al.* Role of hepatitis B virus genotypes and quantitative HBV DNA in metastasis and recurrence of hepatocellular carcinoma. *J Med Virol* 2008; **80**: 591–7.
77 Livingston SE, Simonetti JP, McMahon BJ *et al.* Hepatitis B virus genotypes in Alaska Native people with hepatocellular carcinoma: preponderance of genotype F. *J Infect Dis* 2007; **195**: 5–11.
78 Tseng TC, Kao JH. HBV genotype and clinical outcome of chronic hepatitis B: facts and puzzles. *Gastroenterology* 2008; **134**: 1272–3. author reply 3.
79 Kew MC, Kramvis A, Yu MC, Arakawa K, Hodkinson J. Increased hepatocarcinogenic potential of hepatitis B virus genotype A in Bantu-speaking sub-saharan Africans. *J Med Virol* 2005; **75**: 513–21.
80 Kramvis A, Kew MC, Bukofzer S. Hepatitis B virus precore mutants in serum and liver of Southern African Blacks with hepatocellular carcinoma. *J Hepatol* 1998; **28**: 132–41.
81 Sanchez-Tapias JM, Costa J, Mas A, Bruguera M, Rodes J. Influence of hepatitis B virus genotype on the long-term outcome of chronic hepatitis B in western patients. *Gastroenterology* 2002; **123**: 1848–56.

82 Ou JH, Laub O, Rutter WJ. Hepatitis B virus gene function: the precore region targets the core antigen to cellular membranes and causes the secretion of the e antigen. *Proc Natl Acad Sci U S A* 1986; **83**: 1578–82.
83 Uy A, Bruss V, Gerlich WH, Köchel HG, Thomssen R. Precore sequence of hepatitis B virus inducing e antigen and membrane association of the viral core protein. *Virology* 1986; **155**: 89–96.
84 Miyanohara A, Imamura T, Araki M, Sugawara K, Ohtomo N, Matsubara K. Expression of hepatitis B virus core antigen gene in Saccharomyces cerevisiae: synthesis of two polypeptides translated from different initiation codons. *J Virol* 1986; **59**: 176–80.
85 Kurbanov F, Tanaka Y, Mizokami M. Geographical and genetic diversity of the human hepatitis B virus. *Hepatol Res* 2010; **40**: 14–30.
86 Lindh M, Andersson AS, Gusdal A. Genotypes, nt 1858. variants, and geographic origin of hepatitis B virus – large-scale analysis using a new genotyping method. *J Infect Dis* 1997; **175**: 1285–93.
87 Okamoto H, Tsuda F, Akahane Y *et al.* Hepatitis B virus with mutations in the core promoter for an e antigen-negative phenotype in carriers with antibody to e antigen. *J Virol* 1994; **68**: 8102–10.
88 Buckwold VE, Xu Z, Chen M, Yen TS, Ou JH. Effects of a naturally occurring mutation in the hepatitis B virus basal core promoter on precore gene expression and viral replication. *J Virol* 1996; **70**: 5845–51.
89 Parekh S, Zoulim F, Ahn SH *et al.* Genome replication, virion secretion, and e antigen expression of naturally occurring hepatitis B virus core promoter mutants. *J Virol* 2003; **77**: 6601–12.
90 Kosaka Y, Takase K, Kojima M *et al.* Fulminant hepatitis B: induction by hepatitis B virus mutants defective in the precore region and incapable of encoding e antigen. *Gastroenterology* 1991; **100**: 1087–94.
91 Karayiannis P, Alexopoulou A, Hadziyannis S *et al.* Fulminant hepatitis associated with hepatitis B virus e antigen-negative infection: importance of host factors. *Hepatology* 1995; **22**: 1628–34.
92 Laskus T, Rakela J, Nowicki MJ, Persing DH. Hepatitis B virus core promoter sequence analysis in fulminant and chronic hepatitis B. *Gastroenterology* 1995; **109**: 1618–23.
93 Laskus T, Rakela J, Persing DH. The stem-loop structure of the cis-encapsidation signal is highly conserved in naturally occurring hepatitis B virus variants. *Virology* 1994; **200**: 809–12.
94 Liu CJ, Kao JH, Lai MY, Chen PJ, Chen DS. Precore/core promoter mutations and genotypes of hepatitis B virus in chronic hepatitis B patients with fulminant or subfulminant hepatitis. *J Med Virol* 2004; **72**: 545–50.
95 Pollicino T, Zanetti AR, Cacciola I *et al.* Pre-S2 defective hepatitis B virus infection in patients with fulminant hepatitis. *Hepatology* 1997; **26**: 495–9.
96 Kalinina T, Riu A, Fischer L, Will H, Sterneck M. A dominant hepatitis B virus population defective in virus secretion because of several S-gene mutations from a patient with fulminant hepatitis. *Hepatology* 2001; **34**: 385–94.
97 Bock CT, Tillmann HL, Maschek HJ, Manns MP, Trautwein C. A preS mutation isolated from a patient with chronic hepatitis B infection leads to virus retention and misassembly. *Gastroenterology* 1997; **113**: 1976–82.
98 Zhang K, Imazeki F, Fukai K *et al.* Analysis of the complete hepatitis B virus genome in patients with genotype C chronic hepatitis in relation to HBeAg and anti-HBe. *J Med Virol* 2007; **79**: 683–93.
99 Baptista M, Kramvis A, Kew MC. High prevalence of 1762(T) 1764(A) mutations in the basic core promoter of hepatitis B virus isolated from black Africans with hepatocellular carcinoma compared with asymptomatic carriers. *Hepatology* 1999; **29**: 946–53.
100 Liu CJ, Chen BF, Chen PJ *et al.* Role of hepatitis B virus precore/core promoter mutations and serum viral load on noncirrhotic hepatocellular carcinoma: a case–control study. *J Infect Dis* 2006; **194**: 594–9.
101 Guo X, Jin Y, Qian G, Tu H. Sequential accumulation of the mutations in core promoter of hepatitis B virus is associated with the development of hepatocellular carcinoma in Qidong, China. *J Hepatol* 2008; **49**: 718–25.
102 Tong MJ, Blatt LM, Kao JH, Cheng JT, Corey WG. Basal core promoter T1762/A1764 and precore A1896 gene mutations in hepatitis B surface antigen-positive hepatocellular carcinoma: a comparison with chronic carriers. *Liver Int* 2007; **27**: 1356–63.
103 Tong MJ, Blatt LM, Kao JH, Cheng JT, Corey WG. Precore/basal core promoter mutants and hepatitis B viral DNA levels as predictors for liver deaths and hepatocellular carcinoma. *World J Gastroenterol* 2006; **12**: 6620–6.
104 Yang HI, Yeh SH, Chen PJ *et al.* REVEAL-HBV Study Group. Associations between hepatitis B virus genotype and mutants and the risk of hepatocellular carcinoma. *J Natl Cancer Inst* 2008; **100**: 1134–43.
105 Fang ZL, Sabin CA, Dong BQ *et al.* HBV A1762T, G1764A mutations are a valuable biomarker for identifying a subset of male HBsAg carriers at extremely high risk of hepatocellular carcinoma: a prospective study. *Am J Gastroenterol* 2008; **103**: 2254–62.
106 Bläckberg J, Kidd-Ljunggren K. Mutations within the hepatitis B virus genome among chronic hepatitis B patients with hepatocellular carcinoma. *J Med Virol* 2003; **71**: 18–23.
107 Zhang KY, Imazeki F, Fukai K *et al.* Analysis of the complete hepatitis B virus genome in patients with genotype C chronic hepatitis and hepatocellular carcinoma. *Cancer Sci* 2007; **98**: 1921–9.
108 Fang ZL, Sabin CA, Dong BQ *et al.* Hepatitis B virus pre-S deletion mutations are a risk factor for hepatocellular carcinoma: a matched nested case–control study. *J Gen Virol* 2008; **89**: 2882–90.

109 Chen BF, Liu CJ, Jow GM, Chen PJ, Kao JH, Chen DS. High prevalence and mapping of pre-S deletion in hepatitis B virus carriers with progressive liver diseases. *Gastroenterology* 2006; **130**: 1153–68.
110 Mun HS, Lee SA, Jee Y *et al.* The prevalence of hepatitis B virus preS deletions occurring naturally in Korean patients infected chronically with genotype C. *J Med Virol* 2008; **80**: 1189–94.
111 Takahashi K, Akahane Y, Hino K, Ohta Y, Mishiro S. Hepatitis B virus genomic sequence in the circulation of hepatocellular carcinoma patients: comparative analysis of 40 full-length isolates. *Arch Virol* 1998; **143**: 2313–26.
112 Zanetti AR, Tanzi E, Manzillo G *et al.* Hepatitis B variant in Europe. *Lancet* 1988; **2**: 1132–3.
113 Carman WF, Zanetti AR, Karayiannis P *et al.* Vaccine-induced escape mutant of hepatitis B virus. *Lancet* 1990; **336**: 325–9.
114 Yamamoto K, Horikita M, Tsuda F *et al.* Naturally occurring escape mutants of hepatitis B virus with various mutations in the S gene in carriers seropositive for antibody to hepatitis B surface antigen. *J Virol* 1994; **68**: 2671–6.
115 Hsu HY, Chang MH, Liaw SH, Ni YH, Chen HL. Changes of hepatitis B surface antigen variants in carrier children before and after universal vaccination in Taiwan. *Hepatology* 1999; **30**: 1312–17.
116 McMahon G, Ehrlich PH, Moustafa ZA *et al.* Genetic alterations in the gene encoding the major HBsAg: DNA and immunological analysis of recurrent HBsAg derived from monoclonal antibody-treated liver transplant patients. *Hepatology* 1992; **15**: 757–66.
117 Carman WF, Trautwein C, van Deursen FJ *et al.* Hepatitis B virus envelope variation after transplantation with and without hepatitis B immune globulin prophylaxis. *Hepatology* 1996; **24**: 489–93.
118 Ghany MG, Ayola B, Villamil FG *et al.* Hepatitis B virus S mutants in liver transplant recipients who were reinfected despite hepatitis B immune globulin prophylaxis. *Hepatology* 1998; **27**: 213–22.
119 Jongerius JM, Wester M, Cuypers HT *et al.* New hepatitis B virus mutant form in a blood donor that is undetectable in several hepatitis B surface antigen screening assays. *Transfusion* 1998; **38**: 56–9.
120 Chemin I, Trépo C. Clinical impact of occult HBV infections. *J Clin Virol* 2005; **34** (Suppl 1): S15–21.
121 Torresi J, Earnest-Silveira L, Civitico G *et al.* Restoration of replication phenotype of lamivudine-resistant hepatitis B virus mutants by compensatory changes in the "fingers" subdomain of the viral polymerase selected as a consequence of mutations in the overlapping S gene. *Virology* 2002; **299**: 88–99.
122 Hsu CW, Yeh CT, Chang ML, Liaw YF. Identification of a hepatitis B virus S gene mutant in lamivudine-treated patients experiencing HBsAg seroclearance. *Gastroenterology* 2007; **132**: 543–50.
123 Chu CM, Yeh CT, Tsai SL *et al.* HBsAg seroclearance in asymptomatic carriers of high endemic areas: appreciably high rates during a long-term follow-up. *Hepatology* 2007; **45**: 1187–92.
124 Iloeje UH, Yang HI, Su J *et al.* Predicting cirrhosis risk based on the level of circulating hepatitis B viral load. *Gastroenterology* 2006; **130**: 678–86.
125 Yuen MF, Ng IO, Fan ST *et al.* Significance of HBV DNA levels in liver histology of HBeAg and Anti-HBe positive patients with chronic hepatitis B. *Am J Gastroenterol* 2004; **99**: 2032–7.
126 Lai CL, Chien RN, Leung NW *et al.* A one-year trial of lamivudine for chronic hepatitis B. Asia Hepatitis Lamivudine Study Group. *N Engl J Med* 1998; **339**: 61–8.
127 Hadziyannis SJ, Tassopoulos NC, Heathcote EJ *et al.* Adefovir dipivoxil for the treatment of hepatitis B e antigen-negative chronic hepatitis B. *N Engl J Med* 2003; **348**: 800–7.
128 Marcellin P, Chang TT, Lim SG *et al.* Adefovir dipivoxil for the treatment of hepatitis B e antigen-positive chronic hepatitis B. *N Engl J Med* 2003; **348**: 808–16.
129 Marcellin P, Lau GKK, Bonino F *et al.* Peginterferon alfa-2a alone, lamivudine alone and the two in combination in patients with HBeAg negative chronic hepatitis B. *N Engl J Med* 2004; **351**: 1206–17.
130 Lau GK, Piratvisuth T, Luo KX *et al.* Peginterferon Alfa-2a, lamivudine, and the combination for HBeAg-positive chronic hepatitis B. *N Engl J Med* 2005; **352**: 2682–95.
131 Sherman M, Yurdaydin C, Sollano J *et al.* Entecavir for treatment of lamivudine-refractory, HBeAg-positive chronic hepatitis B. *Gastroenterology* 2006; **130**: 2039–49.
132 Lai CL, Gane E, Liaw YF *et al.* Telbivudine versus lamivudine in patients with chronic hepatitis B. *N Engl J Med* 2007; **357**: 2576–88.
133 Chien RN, Lin CH, Liaw YF. The effect of lamivudine therapy in hepatic decompensation during acute exacerbation of chronic hepatitis B. *J Hepatol* 2003; **38**: 322–7.
134 Liaw YF, Sung JJ, Chow WC *et al.* Lamivudine for patients with chronic hepatitis B and advanced liver disease. *N Engl J Med* 2004; **351**: 1521–31.
135 Leung NW, Lai CL, Chang TT *et al.* Extended lamivudine treatment in patients with chronic hepatitis B enhances hepatitis B e antigen seroconversion rates: results after 3 years of therapy. *Hepatology* 2001; **33**: 1527–32.
136 Liaw YF, Chang TT, Wu SS *et al.* Long-term entecavir therapy results in reversal of fibrosis/cirrhosis and continued histologic improvement in patients with HBeAg(+) and (−) chronic hepatitis B: results from studies ETV-022, -027 and -901. *Hepatology* 2008; **48**: 706A. abst 894.
137 Lok AS, Zoulim F, Locarnini S *et al.* Hepatitis B Virus Drug Resistance Working Group. *Hepatology* 2007; **46**: 254–65.
138 Yuan HJ, Lee WM. Molecular mechanisms of resistance to antiviral therapy in patients with chronic hepatitis B. *Curr Mol Med* 2007; **7**: 185–97.

139 Chang TT, Lai CL, Chien RN *et al.* Four years of lamivudine treatment in Chinese patients with chronic hepatitis B. *J Gastroenterol Hepatol* 2004; **19**: 1276–82.
140 Yatsuji H, Noguchi C, Hiraga N *et al.* Emergence of a novel lamivudine-resistant hepatitis B virus variant with a substitution outside the YMDD motif. *Antimicrob Agents Chemother* 2006; **50**: 3867–74.
141 Gaia S, Marzano A, Smedile A *et al.* Four years of treatment with lamivudine: clinical and virological evaluations in HBe antigen-negative chronic hepatitis B. *Aliment Pharmacol Ther* 2004; **20**: 281–7.
142 Tipples GA, Ma MM, Fischer KP, Bain VG, Kneteman NM, Tyrrell DL. Mutation in HBV RNA-dependent DNA polymerase confers resistance to lamivudine *in vivo*. *Hepatology* 1996; **24**: 714–17.
143 Chayama K, Suzuki Y, Kobayashi M *et al.* Emergence and takeover of YMDD motif mutant hepatitis B virus during long-term lamivudine therapy and re-takeover by wild type after cessation of therapy. *Hepatology* 1998; **27**: 1711–16.
144 Matsumoto A, Tanaka E, Rokuhara A *et al.* Efficacy of lamivudine for preventing hepatocellular carcinoma in chronic hepatitis B: a multicenter retrospective study of 2795 patients. *Hepatol Res* 2005; **32**: 173–84.
145 Ono-Nita SK, Kato N, Shiratori Y *et al.* YMDD motif in hepatitis B virus DNA polymerase influences on replication and lamivudine resistance: a study by *in vitro* full-length viral DNA transfection. *Hepatology* 1999; **29**: 939–45.
146 Lok AS, Hussain M, Cursano C *et al.* Evolution of hepatitis B virus polymerase gene mutations in hepatitis B e antigen-negative patients receiving lamivudine therapy. *Hepatology* 2000; **32**: 1145–53.
147 Ono-Nita SK, Kato N, Shiratori Y *et al.* Susceptibility of lamivudine-resistant hepatitis B virus to other reverse transcriptase inhibitors. *J Clin Invest* 1999; **103**: 1635–40.
148 Delaney WE 4th, Yang H, Westland CE *et al.* The hepatitis B virus polymerase mutation rtV173L is selected during lamivudine therapy and enhances viral replication *in vitro*. *J Virol* 2003; **77**: 11833–41.
149 Zollner B, Petersen J, Schafer P *et al.* Subtype-dependent response of hepatitis B virus during the early phase of lamivudine treatment. *Clin Infect Dis* 2002; **34**: 1273–7.
150 Kobayashi M, Akuta N, Suzuki F *et al.* Virological outcomes in patients infected chronically with hepatitis B virus genotype A in comparison with genotypes B and C. *J Med Virol* 2006; **78**: 60–7.
151 Yeh CT, Chien RN, Chu CM, Liaw YF. Clearance of the original hepatitis B virus YMDD-motif mutants with emergence of distinct lamivudine-resistant mutants during prolonged lamivudine therapy. *Hepatology* 2000; **31**: 1318–26.
152 Fung SK, Chae HB, Fontana RJ *et al.* Virologic response and resistance to adefovir in patients with chronic hepatitis B. *J Hepatol* 2006; **44**: 283–90.
153 Hadziyannis SJ, Tassopoulos NC, Heathcote EJ *et al.* Adefovir Dipivoxil 438 Study Group.Long-term therapy with adefovir dipivoxil for HBeAg-negative chronic hepatitis B. *N Engl J Med* 2005; **352**: 2673–81.
154 Hadziyannis SJ, Tassopoulos NC, Heathcote EJ *et al.* Adefovir Dipivoxil 438 Study Group. Long-term therapy with adefovir dipivoxil for HBeAg-negative chronic hepatitis B for up to 5 years. *Gastroenterology* 2006; **131**: 1743–51.
155 Angus P, Vaughan R, Xiong S *et al.* Resistance to adefovir dipivoxil therapy associated with the selection of a novel mutation in the HBV polymerase. *Gastroenterology* 2003; **125**: 292–7.
156 Lee YS, Suh DJ, Lim YS *et al.* Increased risk of adefovir resistance in patients with lamivudine-resistant chronic hepatitis B after 48 weeks of adefovir dipivoxil monotherapy. *Hepatology* 2006; **43**: 1385–91.
157 Chen CH, Wang JH, Lee CM *et al.* Virological response and incidence of adefovir resistance in lamivudine-resistant patients treated with adefovir dipivoxil. *Antivir Ther* 2006; **11**: 771–8.
158 Yeon JE, Yoo W, Hong SP *et al.* Resistance to adefovir dipivoxil in lamivudine resistant chronic hepatitis B patients treated with adefovir dipivoxil. *Gut* 2006; **55**: 1488–95.
159 Chang TT, Gish RG, de Man R *et al.* BEHoLD AI463022 Study Group A comparison of entecavir and lamivudine for HBeAg-positive chronic hepatitis B. *N Engl J Med* 2006; **354**: 1001–10.
160 Tenney DJ, Rose RE, Baldick CJ *et al.* Long-term monitoring shows hepatitis B virus resistance to entecavir in nucleoside-naïve patients is rare through 5 years of therapy. *Hepatology* 2009; **49**: 1503–14.
161 Lai CL, Shouval D, Lok AS *et al.* BEHoLD AI463027 Study Group. Entecavir versus lamivudine for patients with HBeAg-negative chronic hepatitis B. *N Engl J Med* 2006; **9** (354): 1011–20.
162 Innaimo SF, Seifer M, Bisacchi GS, Standring DN, Zahler R, Colonno RJ. Identification of BMS-200475 as a potent and selective inhibitor of hepatitis B virus. *Antimicrob Agents Chemother* 1997; **41**: 1444–8.
163 Colonno RJ, Rose R, Baldick CJ *et al.* Entecavir resistance is rare in nucleoside naïve patients with hepatitis B. *Hepatology* 2006; **44**: 1656–65.
164 Tenney DJ, Rose RE, Baldick CJ *et al.* Two-year assessment of entecavir resistance in Lamivudine-refractory hepatitis B virus patients reveals different clinical outcomes depending on the resistance substitutions present. *Antimicrob Agents Chemother* 2007; **51**: 902–11.
165 Suzuki F, Suzuki Y, Akuta N *et al.* Changes in viral loads of lamivudine-resistant mutants during entecavir therapy. *Hepatol Res* 2008; **9** (38): 132–40.
166 Hoofnagle JH, Peters M, Mullen KD *et al.* Randomized, controlled trial of recombinant human alpha-interferon in patients with chronic hepatitis B. *Gastroenterology* 1988; **95**: 1318–25.

167 Perrillo RP, Schiff ER, Davis GL *et al.* A randomized, controlled trial of interferon alfa-2b alone and after prednisone withdrawal for the treatment of chronic hepatitis B. The Hepatitis Interventional Therapy Group. *N Engl J Med* 1990; **323**: 295–301.
168 Suzuki F, Arase Y, Akuta N *et al.* Efficacy of 6-month interferon therapy in chronic hepatitis B virus infection in Japan. *J Gastroenterol* 2004; **39**: 969–74.
169 Zhao H, Kurbanov F, Wan MB *et al.* Genotype B and younger patient age associated with better response to low-dose therapy: a trial with pegylated/nonpegylated interferon-alpha-2b for hepatitis B e antigen-positive patients with chronic hepatitis B in China. *Clin Infect Dis* 2007; **44**: 541–8.
170 Janssen HL, van Zonneveld M, Senturk H *et al.* Pegylated interferon alfa-2b alone or in combination with lamivudine for HBeAg-positive chronic hepatitis B: a randomised trial. *Lancet* 2005; **365**: 123–9.
171 Perrillo R, Tamburro C, Regenstein F *et al.* Low-dose, titratable interferon alfa in decompensated liver disease caused by chronic infection with hepatitis B virus. *Gastroenterology* 1995; **109**: 908–16.
172 Hoofnagle JH, Di Bisceglie AM, Waggoner JG, Park Y. Interferon alfa for patients with clinically apparent cirrhosis due to chronic hepatitis B. *Gastroenterology* 1993; **104**: 1116–21.
173 Wong DK, Cheung AM, O'Rourke K, Naylor CD, Detsky AS, Heathcote J. Effect of alpha-interferon treatment in patients with hepatitis B e antigen-positive chronic hepatitis B. A meta-analysis. *Ann Intern Med* 1993; **119**: 312–23.
174 Janssen HL, Gerken G, Carreno V *et al.* Interferon alfa for chronic hepatitis B infection: increased efficacy of prolonged treatment. The European Concerted Action on Viral Hepatitis (EUROHEP). *Hepatology* 1999; **30**: 238–43.
175 Niederau C, Heintges T, Lange S *et al.* Long-term follow-up of HBeAg-positive patients treated with interferon alfa for chronic hepatitis B. *N Engl J Med* 1996; **334**: 1422–7.
176 Lok AS, Chung HT, Liu VW, Ma OC. Long-term follow-up of chronic hepatitis B patients treated with interferon alfa. *Gastroenterology* 1993; **105**: 1833–8.
177 Lin SM, Tai DI, Chien RN, Sheen IS, Chu CM, Liaw YF. Comparison of long-term effects of lymphoblastoid interferon alpha and recombinant interferon alpha-2a therapy in patients with chronic hepatitis B. *J Viral Hepat* 2004; **11**: 349–57.
178 Fattovich G, Giustina G, Realdi G, Corrocher R, Schalm SW. Long-term outcome of hepatitis B e antigen-positive patients with compensated cirrhosis treated with interferon alfa. European Concerted Action on Viral Hepatitis (EUROHEP). *Hepatology* 1997; **26**: 1338–42.
179 Fattovich G, Farci P, Rugge M *et al.* A randomized controlled trial of lymphoblastoid interferon-alpha in patients with chronic hepatitis B lacking HBeAg. *Hepatology* 1992; **15**: 584–9.
180 Hadziyannis S, Bramou T, Makris A, Moussoulis G, Zignego L, Papaioannou C. Interferon alfa-2b treatment of HBeAg negative/serum HBV DNA positive chronic active hepatitis type B. *J Hepatol* 1990; **11** (Suppl 1): S133–136.
181 Papatheodoridis GV, Manesis E, Hadziyannis SJ. The long-term outcome of interferon-alpha treated and untreated patients with HBeAg-negative chronic hepatitis B. *J Hepatol* 2001; **34**: 306–13.
182 Brunetto MR, Oliveri F, Coco B *et al.* Outcome of anti-HBe positive chronic hepatitis B in alpha-interferon treated and untreated patients: a long term cohort study. *J Hepatol* 2002; **36**: 263–70.
183 Manesis EK, Hadziyannis SJ. Interferon alpha treatment and retreatment of hepatitis B e antigen-negative chronic hepatitis B. *Gastroenterology* 2001; **121**: 101–9.
184 Lampertico P, Del Ninno E, Vigano M *et al.* Long-term suppression of hepatitis B e antigen-negative chronic hepatitis B by 24-month interferon therapy. *Hepatology* 2003; **37**: 756–63.
185 Cooksley WG, Piratvisuth T, Lee SD *et al.* Peginterferon alpha-2a (40 kDa): an advance in the treatment of hepatitis B e antigen-positive chronic hepatitis B. *J Viral Hepat* 2003; **10**: 298–305.
186 Kao JH, Wu NH, Chen PJ, Lai MY, Chen DS. Hepatitis B genotypes and the response to interferon therapy. *J Hepatol* 2000; **33**: 998–1002.
187 Wai CT, Chu CJ, Hussain M, Lok AS. HBV genotype B is associated with better response to interferon therapy in HBeAg(+) chronic hepatitis than genotype C. *Hepatology* 2002; **36**: 1425–30.
188 Flink HJ, van Zonneveld M, Hansen BE, de Man RA, Schalm SW, Janssen HL. Treatment with Peg-interferon alpha-2b for HBeAg-positive chronic hepatitis B: HBsAg loss is associated with HBV genotype. *Am J Gastroenterol* 2006; **101**: 297–303.
189 Buster EH, Flink HJ, Cakaloglu Y *et al.* Sustained HBeAg and HBsAg loss after long-term follow-up of HBeAg-positive patients treated with peginterferon alpha-2b. *Gastroenterology* 2008; **135**: 459–67.
190 Manesis EK, Papatheodoridis GV, Hadziyannis SJ. A partially overlapping treatment course with lamivudine and interferon in hepatitis B e antigen-negative chronic hepatitis B. *Aliment Pharmacol Ther* 2006; **23**: 99–106.
191 Shi M, Wang RS, Zhang H *et al.* Sequential treatment with lamivudine and interferon-alpha monotherapies in hepatitis B e antigen-negative Chinese patients and its suppression of lamivudine-resistant mutations. *J Antimicrob Chemother* 2006; **58**: 1031–5.
192 Schalm SW, Heathcote J, Cianciara J *et al.* Lamivudine and alpha interferon combination treatment of patients with chronic hepatitis B infection: a randomised trial. *Gut* 2000; **46**: 562–8.

193 Yurdaydin C, Bozkaya H, Cetinkaya H *et al.* Lamivudine vs lamivudine and interferon combination treatment of HBeAg(-) chronic hepatitis B. *J Viral Hepat* 2005; **12**: 262–8.
194 Sarin SK, Kumar M, Kumar R *et al.* Higher efficacy of sequential therapy with interferon-alpha and lamivudine combination compared to lamivudine monotherapy in HBeAg positive chronic hepatitis B patients. *Am J Gastroenterol* 2005; **100**: 2463–71.
195 Yang YF, Zhao W, Zhong YD, Xia HM, Shen L, Zhang N. Interferon therapy in chronic hepatitis B reduces progression to cirrhosis and hepatocellular carcinoma: a meta-analysis. *J Viral Hepat* 2009; **16**: 265–2671.
196 Lin SM, Sheen IS, Chien RN *et al.* Long-term beneficial effect of interferon therapy in patients with chronic hepatitis B virus infection. *Hepatology* 1999; **29**: 971–5.
197 van Zonneveld M, Honkoop P, Hansen BE *et al.* Long-term follow-up of alpha-interferon treatment of patients with chronic hepatitis B. *Hepatology* 2004; **39**: 804–10.

J Gastroenterol (2010) 45:1263–1271
DOI 10.1007/s00535-010-0277-6

ORIGINAL ARTICLE—LIVER, PANCREAS, AND BILIARY TRACT

# Accurate and simple method for quantification of hepatic fat content using magnetic resonance imaging: a prospective study in biopsy-proven nonalcoholic fatty liver disease

**Tomoko Hatta · Yasunari Fujinaga · Masumi Kadoya · Hitoshi Ueda · Hiroaki Murayama · Masahiro Kurozumi · Kazuhiko Ueda · Michiharu Komatsu · Tadanobu Nagaya · Satoru Joshita · Ryo Kodama · Eiji Tanaka · Tsuyoshi Uehara · Kenji Sano · Naoki Tanaka**

Received: 6 January 2010 / Accepted: 14 June 2010 / Published online: 13 July 2010


## Abstract

*Background* To assess the degree of hepatic fat content, simple and noninvasive methods with high objectivity and reproducibility are required. Magnetic resonance imaging (MRI) is one such candidate, although its accuracy remains unclear. We aimed to validate an MRI method for quantifying hepatic fat content by calibrating MRI reading with a phantom and comparing MRI measurements in human subjects with estimates of liver fat content in liver biopsy specimens.

*Methods* The MRI method was performed by a combination of MRI calibration using a phantom and double-echo chemical shift gradient-echo sequence (double-echo fast low-angle shot sequence) that has been widely used on a 1.5-T scanner. Liver fat content in patients with nonalcoholic fatty liver disease (NAFLD, $n = 26$) was derived from a calibration curve generated by scanning the phantom. Liver fat was also estimated by optical image analysis. The correlation between the MRI measurements and liver histology findings was examined prospectively.

*Results* Magnetic resonance imaging measurements showed a strong correlation with liver fat content estimated from the results of light microscopic examination (correlation coefficient 0.91, $P < 0.001$) regardless of the degree of hepatic steatosis. Moreover, the severity of lobular inflammation or fibrosis did not influence the MRI measurements.

*Conclusions* This MRI method is simple and noninvasive, has excellent ability to quantify hepatic fat content even in NAFLD patients with mild steatosis or advanced fibrosis, and can be performed easily without special devices.

**Keywords** Fatty liver · Magnetic resonance imaging · Water–oil phantom · Liver biopsy

T. Hatta · Y. Fujinaga · M. Kadoya (✉) · M. Kurozumi · K. Ueda
Department of Radiology, Shinshu University School of Medicine, 3-1-1 Asahi, Matsumoto 390-8621, Japan
e-mail: kadoyam@shinshu-u.ac.jp

H. Ueda · H. Murayama
Section of Radiology, Shinshu University Hospital, Matsumoto, Japan

M. Komatsu · T. Nagaya · S. Joshita · R. Kodama · E. Tanaka · N. Tanaka
Department of Gastroenterology, Shinshu University School of Medicine, Matsumoto, Japan

T. Uehara · K. Sano
Section of Laboratory Medicine, Shinshu University Hospital, Matsumoto, Japan

N. Tanaka
Department of Metabolic Regulation, Shinshu University Graduate School of Medicine, Matsumoto, Japan

## Introduction

Recently, the prevalence of nonalcoholic fatty liver disease (NAFLD) has been increasing throughout the world, with NAFLD considered to be a common cause of chronic liver disease in Western countries, as well as in Japan [1–6]. NAFLD exhibits a wide spectrum ranging from simple steatosis to nonalcoholic steatohepatitis (NASH). NASH is a histological condition characterized by fatty infiltration of the liver, hepatocyte ballooning, lobular inflammation, and perisinusoidal fibrosis [1–3, 5, 7, 8], and the degree of hepatic steatosis is one of the essential components used to evaluate the histological activity of NASH. Thus, it is

important to correctly know the degree of fatty infiltration when we assess therapeutic effects in NAFLD/NASH patients.

Liver biopsy is currently considered as the gold standard for the assessment of NAFLD/NASH, but its invasive nature makes does not justify repeated biopsies to study the natural history of NAFLD or the response to therapeutic interventions for NAFLD. Furthermore, the large numbers of NAFLD patients means that the routine use of liver biopsy in this context is unrealistic. Additionally, liver biopsy is subject to the risk of sampling error, especially in patients with advanced NASH, which shows severe fibrosis and heterogeneously distributed fatty infiltration in the liver. Hence, a simple, accurate, and noninvasive method to assess temporal changes in fatty infiltration of the liver is strongly desired.

Radiological imaging studies such as ultrasonography (US), computed tomography (CT), and magnetic resonance imaging (MRI) have so far been employed as noninvasive methods for assessing hepatic steatosis [2, 3, 9–11]. US is a simple and common examination modality, but is subject to technician-related bias. CT is able to assess fatty deposition objectively, but exposes the patient to radiation. In addition, according to the study of Saadeh et al. [11], CT and US have low sensitivity, of <33%, in the case of fatty infiltration, and these modalities may miss some cases of mild steatosis. On the other hand, MRI has better objectivity and has the advantage of no radiation exposure. Moreover, MRI has a greater ability to differentiate tissue characterization than US and CT, thereby facilitating the detection of slighter degrees of fatty infiltration of the liver [11–16].

Of all MRI techniques, the double-echo chemical shift gradient-echo technique is the most sensitive to detect fat [14, 15, 17–23], and many studies have used this technique to evaluate hepatic steatosis. However, these studies lacked a basic experiment using a phantom or quantitative evaluation in the histopathological assessment of hepatic fat content, or a prospective study design, and were semiquantitative in nature because of the inclusion of a classification of the fat content rate.

Against this background, we formulated a simple and accurate MRI method to quantify the degree of fatty infiltration of the liver, using double-echo chemical shift gradient-echo sequence [double-echo fast low-angle shot (FLASH) sequence] on a 1.5-T scanner. This method does not require specialized software or hardware. For this investigation, we designed a 3-step process comprising: (1) a basic experiment using a phantom, (2) a prospective clinical study using liver biopsy specimens, and (3) quantitative histopathological estimation of liver fat by optical image analysis using commercial software. Furthermore, we sought to demonstrate the accuracy and usefulness of this convenient method for quantifying liver fat content by comparing the MRI measurements with liver fat content calculated by light microscopic findings in patients with biopsy-proven NAFLD.

## Methods

### Theory

The principle of diagnosing hepatic steatosis by double-echo chemical shift gradient-echo MRI is based on the utilization of the difference in the precessional frequency between water and fat protons [12–15]. At 1.5-T, fat protons precess in the *xy*-plane at a rotational velocity 225 Hz, slower than that of water protons. This translates into one less rotation every 4.4 ms or one-half rotation difference every 2.2 ms. In chemical shift imaging, the difference in resonance frequency of water and fat is exploited to create "in-phase (IP)" and "opposed-phase (OP)" images (Fig. 1). By varying the time between excitation and signal acquisition in gradient echo imaging, the magnetic moments of fat and water can be manipulated to lie in either parallel (IP) or anti-parallel (OP) positions. In voxels (volume elements of an MR image) containing a mixture of fat and water, magnetic moment cancellation occurs for OP (but not for IP) images. Thus, a measurable loss of signal in an OP image relative to that of an IP image indicates the presence of voxels containing both water and fat.

### MRI technique

All MR scans were performed with one of two 1.5-T scanners (Symphony or Avanto; Siemens, Erlangen,

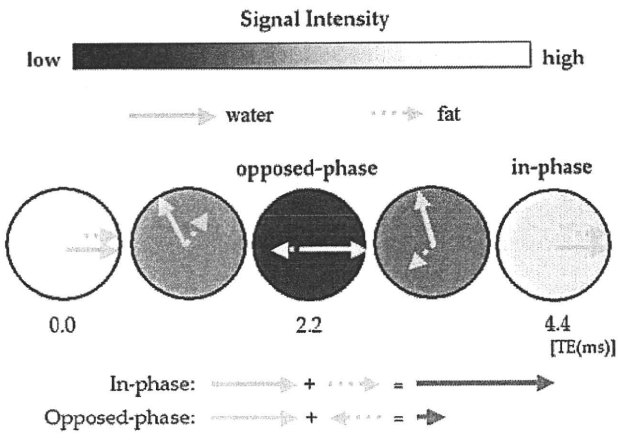


**Fig. 1** Schematic diagram demonstrating the principle of chemical shift imaging. With in-phase imaging (TE = 4.4 ms), the water and fat vectors are aligned, and the total signal intensity is additive. In opposed-phase imaging (TE = 2.2 ms), the vectors lie anti-parallel, resulting in partial signal cancellation by vector addition

Germany) with a body-array coil. All software used for the study was included in scanners as standard equipment.

An in vitro phantom (water–oil phantom) was used to establish a calibration of fat determination based on the double-echo FLASH technique. An in vivo study, using this phantom calibration and the same MRI methodology, was then performed to assess liver fat content in patients.

For the phantom study, double-echo FLASH imaging was performed with a repetition time (TR) of 100 ms, double echo times (TEs) of 2.2 ms for OP and 4.4 ms for IP, flip angle of 80° (Avanto) and 90° (Symphony), slice thickness of 5 mm, 32 × 32 cm field of view, and 320 × 320 matrix, with the use of a body-array coil.

For the clinical study, MR scans were performed with TRs of 145 ms (Avanto) and 80–103 ms (Symphony), TEs of 2.2 and 4.4 ms (both Avanto and Symphony), and a flip angle of 80° (Avanto) and 90° (Symphony), and 256 × (256–192) matrix, and the field of view was increased to 26 × 26 cm–34 × 34 cm depending on the patient size, with a body-array coil. Transverse images were obtained with a 6-mm slice thickness and a 2-mm inter-slice gap.

Study 1 (phantom study)

We used a phantom model that consisted of a test tube filled with water (physiological saline; Otsuka, Tokyo, Japan) and mineral oil (Johnson's baby oil; Johnson & Johnson, New Brunswick, NJ, USA). The oil was layered on water, which provided an oil–water interface in which to test various fractions of fat to water (Fig. 2). Imaging of the water–oil phantom was repeated with the phantom in a horizontal position. Six sections that were each composed of 5-mm-thick slices were obtained parallel to the water–oil interface by using the double-echo FLASH sequence. The location of the six sections was then processed in increments of 0.5 mm at a time to create a stepwise quantifiable transition across the water–oil interface [i.e., from 0 to 50% oil (in increments of 10%) in each slice, respectively].

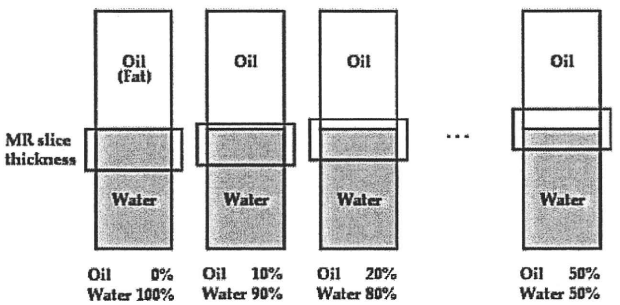


**Fig. 2** Schematic presentation of a water–oil phantom. The water–oil phantom using physiological saline water was layered with mineral oil, which provided a water–oil interface in which to test various fractions of fat to water. Images were obtained in the transverse plane from the bottom (0% oil) to the top (50% oil) of the phantom for various proportions of fat and water protons within each voxel. *MR* Magnetic resonance

Data were analyzed using a region of interest (ROI) of 9.8 $cm^2$ on each IP and OP image. Data acquisition was repeated three times, and the average value of three measurements was appropriated to a calibration reference for liver fat quantification.

Quantitative measurement of signal intensity (SI) changes between IP and OP images was calculated as follows: the SI ratio = $SI_{op}/SI_{in}$, where $SI_{in}$ is SI measured on IP images and $SI_{op}$ is SI measured on OP images. The SI ratio was plotted against known fat percentages and the data were fitted to a polynomial function using Microsoft Office Excel 2003 (Microsoft, Redmond, WA, USA), which served as a calibration reference for hepatic fat quantification.

Study 2 (clinical study)

The study protocol was approved by the Committee for Medical Ethics of Shinshu University School of Medicine (the approved ID number is 927). Informed consent was obtained from all patients.

For validation analysis, 26 consecutive patients with NAFLD were enrolled (12 men, 14 women; mean age 44.7 years; range 20–80 years). The possibility of NAFLD was considered according to the following criteria: (1) the presence of hepatorenal contrast and increased hepatic echogenicity on abdominal US; (2) no consumption of alcohol; and (3) the absence of other causes of liver dysfunction such as chronic viral hepatitis, drug-induced liver injury, autoimmune liver disease, primary biliary cirrhosis, primary sclerosing cholangitis, Wilson's disease, hereditary hemochromatosis, and α1-antitrypsin deficiency. The diagnosis of NAFLD/NASH was confirmed by US-guided percutaneous liver biopsy. The histological activity and severity of NAFLD were assessed by an independent pathologist (K.S.) in a blinded fashion according to the scoring system proposed by Kleiner et al. [5]. NASH was defined as the presence of macrovesicular steatosis (>5% of hepatocytes affected), hepatocyte ballooning, and lobular inflammation.

Body height and weight were measured before liver biopsy, in the fasting state, and any underlying diseases, medical interventions, and past medical history were also recorded. The presence of obesity was defined as having a body mass index (BMI) of more than 25 $kg/m^2$, based on criteria released by the Japan Society for the Study of Obesity [24]. Patients were considered hypertensive if their systolic/diastolic pressure was >140/90 mmHg, or if they were taking antihypertensive drugs. Patients were

considered to have hyperlipidemia if their fasting serum levels of cholesterol and triglycerides were equal to or higher than 220 and 150 mg/dL, respectively, or if they were taking lipid-lowering drugs [25–27]. All laboratory data were obtained in a fasting state before liver biopsy.

All patients had an MRI scan immediately before US-guided percutaneous liver biopsy. The MR images were analyzed with a commercial software package, EV client (PSP, Tokyo, Japan). Using this software, we can set out an ROI in the same location and the same area for each IP and OP image pair (Fig. 3). For each case, hepatic SI was measured by three oval ROIs that were selected in the anterior segment of the right lobe of the liver in three slices in an effort to include the biopsy area, and were placed in the liver parenchyma to exclude contamination from blood vessels, motion artifacts, or partial volume effects. The areas of these ROIs varied between 269 and 1501 $mm^2$ because the ROIs were set apart from large vessels.

Mean pixel SI levels for each ROI were used to calculate the SI ratio. The SI ratio within the ROI was entered into the polynomial function representing the calibration curve, and a measurement of hepatic fat content was obtained by solving the equation.

## Histopathological analysis

Liver biopsy specimens were obtained from segment 5 or 8 using 14-G needles and immediately fixed in 10% neutral formalin. Sections were cut at 4-μm thickness and stained using hematoxylin and eosin and Azan–Mallory methods.

Digital images of hematoxylin and eosin-stained liver biopsy sections were converted into a gray scale, and evaluated to maximize the contrast between fat droplets and hepatocytes, connective tissue, and vascular or biliary structures (Fig. 4). PhotoShop 7.0 (Adobe, San Jose, CA, USA) was used to inspect the digital images and to count the total number of pixels corresponding to fat globules. The total number of pixels corresponding to fat globules was divided by the total number of pixels in an entire field to calculate the area fraction representing fat. Twenty microscopic fields (400×) of each case were selected at random, and the fat fraction of each field was measured. The average of the measurements for all 20 fields was used as the representative liver fat content of each patient.

In addition, hepatic iron deposition that was identified with Perls' Prussian blue stain was evaluated in all biopsy specimens. The severity of iron deposition was classified

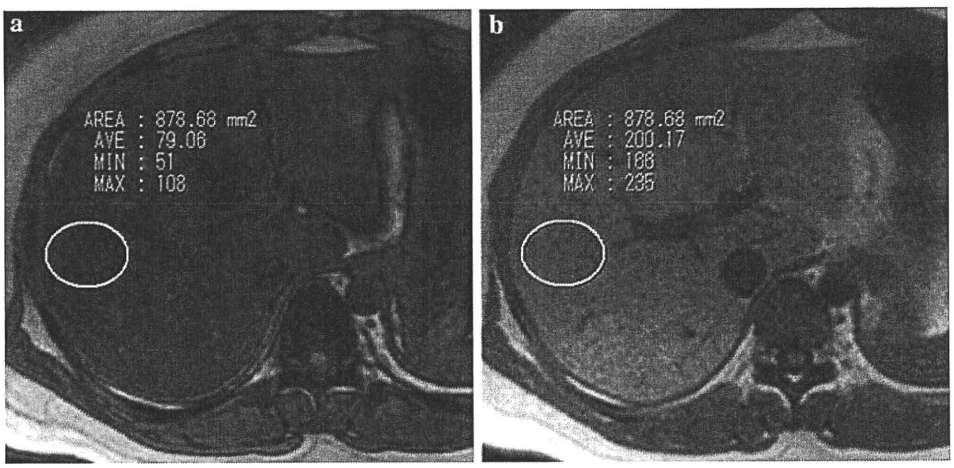


**Fig. 3** Quantitation of hepatic fat using magnetic resonance imaging (MRI). MR images of the liver were obtained with **a** opposed-phase and **b** in-phase technique. The regions of interest drawn on each image (*circles*) measure the mean signal intensities of all cases

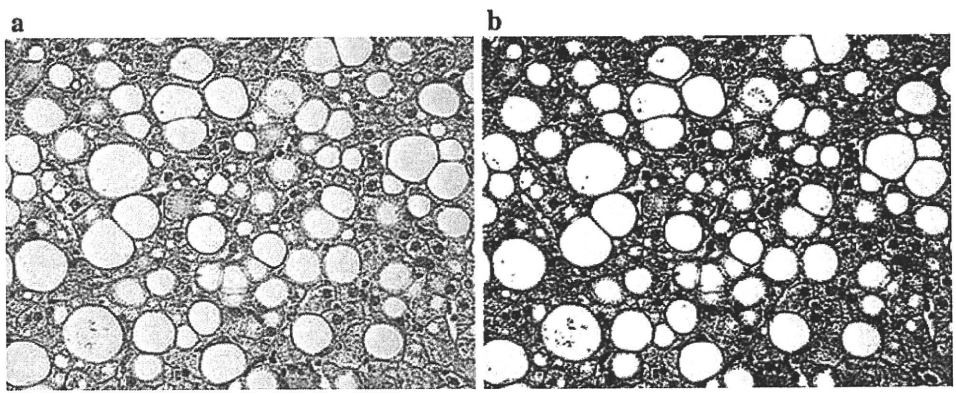


**Fig. 4** Digital images of H&E-stained liver biopsy sections (400×) were converted into a gray scale (**a**), and evaluated to maximize the contrast between fat globules and liver and connective tissue (**b**)

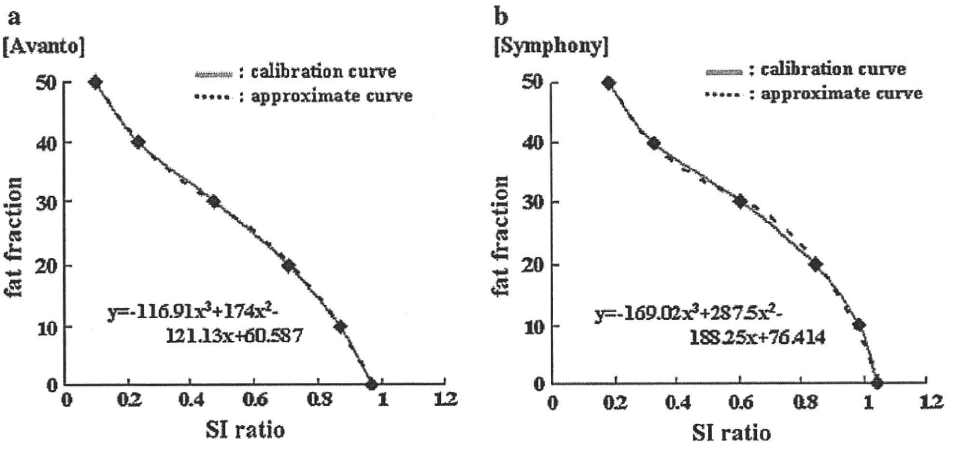


**Fig. 5** The fat fractions versus signal intensity (*SI*) ratio measurements with the phantom and the approximate curve derived from the phantom data ([a Avanto] and [b Symphony])

into five grades according to a previous report [28], as follows: grade 0, granules were absent or barely discernible at 400× magnification; grade 1, granules were barely discernible at 250× magnification or were easily confirmed at 400× magnification; grade 2, discrete granules were visible at 100× magnification; grade 3, discrete granules were visible at 25× magnification; and grade 4, masses were visible at 10× magnification or with visual observation.

### Statistical analysis

Statistical analysis was performed with Microsoft Excel 2003 (Microsoft). Linear regression analysis and the Pearson's correlation coefficient were used to examine the association between MRI measurements and optical image analysis results. Data were expressed as means ± standard error (SE). In addition, we analyzed the effects of significant fibrosis (stage 2–4) or lobular inflammation (score 2 and 3) on the correlation between the MRI measurements and optical image analysis results. A value of $P < 0.05$ was considered to indicate a statistically significant difference.

## Results

### Study 1 (phantom study)

The fat fractions versus SI ratio measurements with the phantom are plotted in Fig. 5. The association between the mean SI ratio and fat content was well approximated by a cubic polynomial function, independently of the degree of fat fractions. This result suggests that substituting the SI ratio obtained from this MRI method can reflect the actual hepatic fat content.

### Study 2 (clinical study)

To examine whether this system can be applied to the measurement of hepatic fat content in vivo, MRI measurements were performed in 26 NAFLD patients just before liver biopsy and compared with the histological findings. The baseline characteristics of the patients and the liver biopsy findings are summarized in Tables 1 and 2, respectively. Twenty-one patients (81%) had obesity, and 15 (58%) were diagnosed as having NASH.

**Table 1** Baseline characteristics of the patients

| Parameter | Mean ± SD or *n* |
|---|---|
| Age (years) | 44.7 ± 16.4 |
| Female | 14 (54%) |
| Obesity | 21 (81%) |
| Diabetes | 6 (23%) |
| Hypertension | 3 (12%) |
| Hyperlipidemia | 9 (35%) |
| BMI (kg/m$^2$) | 28.4 ± 4.4 |
| Platelets (×10$^3$/μL) | 245 ± 70 |
| ALT (IU/L) | 85 ± 59 |
| AST (IU/L) | 53 ± 31 |
| γGT (IU/L) | 71 ± 59 |
| Total cholesterol (mg/dL) | 222 ± 44 |
| Triglycerides (mg/dL) | 161 ± 86 |
| HDL-C (mg/dL) | 54 ± 10 |
| FPG (mg/dL) | 109 ± 23 |
| IRI (μU/mL) | 18 ± 12 |
| HbA1c (%) | 5.8 ± 1.0 |
| HOMA-IR | 5.2 ± 4.0 |
| Iron (μg/dL) | 120 ± 37 |
| Transferrin saturation (%) | 32.8 ± 12.9 |
| Ferritin (ng/mL) | 172 ± 176 |

Quantitative data are expressed as means and standard deviation (SD), and qualitative data are expressed as percentages

*BMI* Body mass index, *ALT* alanine aminotransferase, *AST* aspartate aminotransferase, *γGT* γ-glutamyltransferase, *HDL-C* high-density lipoprotein cholesterol, *FPG* fasting plasma glucose, *IRI* immunoreactive insulin, *HOMA-IR* homeostasis model assessment of insulin resistance

**Table 2** Histological activity and severity, and fat content determined by optical imaging analysis and magnetic resonance imaging (MRI) in the patients

| Patient no. | Macrovesicular steatosis | Fibrosis | Lobular Inflammation | Ballooning | NAS | % Fat by optical imaging | % Fat by MR imaging |
|---|---|---|---|---|---|---|---|
| 1 | 3 | 1A | 2 | 1 | 5 | 38.6 | 43.2 |
| 2 | 1 | 1A | 1 | 0 | 2 | 15.9 | 23.2 |
| 3 | 1 | 1A | 1 | 0 | 2 | 16.4 | 19.2 |
| 4 | 1 | 1A | 1 | 1 | 3 | 20.6 | 27.0 |
| 5 | 1 | 1A | 1 | 1 | 3 | 25.3 | 24.2 |
| 6 | 2 | 1A | 2 | 1 | 5 | 24.3 | 27.6 |
| 7 | 3 | 1A | 3 | 2 | 7 | 32.8 | 35.4 |
| 8 | 1 | 2 | 1 | 0 | 1 | 3.8 | 5.0 |
| 9 | 3 | 1A | 2 | 2 | 7 | 29.6 | 34.7 |
| 10 | 2 | 1A | 1 | 0 | 3 | 18.1 | 22.4 |
| 11 | 2 | 1A | 2 | 0 | 4 | 29.1 | 29.7 |
| 12 | 2 | 0 | 1 | 0 | 3 | 30.2 | 30.3 |
| 13 | 1 | 3 | 2 | 2 | 5 | 9.3 | 10.3 |
| 14 | 3 | 0 | 1 | 1 | 5 | 33.5 | 36.7 |
| 15 | 1 | 1A | 3 | 1 | 5 | 19.8 | 21.0 |
| 16 | 1 | 1A | 1 | 0 | 2 | 12.5 | 14.7 |
| 17 | 2 | 2 | 2 | 2 | 6 | 21.2 | 24.2 |
| 18 | 1 | 3 | 2 | 1 | 4 | 6.2 | 6.7 |
| 19 | 2 | 1A | 2 | 1 | 5 | 20.0 | 22.0 |
| 20 | 2 | 0 | 2 | 1 | 5 | 20.6 | 27.4 |
| 21 | 3 | 0 | 1 | 1 | 5 | 30.7 | 31.3 |
| 22 | 3 | 2 | 3 | 2 | 8 | 27.7 | 21.2 |
| 23 | 1 | 0 | 1 | 0 | 2 | 18.6 | 9.9 |
| 24 | 2 | 2 | 3 | 1 | 6 | 18.3 | 15.2 |
| 25 | 1 | 0 | 1 | 1 | 3 | 14.1 | 14.8 |
| 26 | 2 | 0 | 1 | 0 | 3 | 23.6 | 18.4 |

Histological findings were scored according to criteria proposed by Kleiner et al. [5]

*NAS* nonalcoholic fatty liver disease activity score

The results of the optical image analysis and the MRI determined percentage of fat for all patients were 21.5 ± 8.6 and 22.9 ± 9.5%, respectively. The MRI measurements were significantly correlated with the estimates of liver fat content made by optical image analysis (Fig. 6, $r = 0.91$, $P < 0.001$). In addition, even in patients with mild steatosis (5–33% of hepatocytes affected), the MRI measurements correlated well with the estimates ($r = 0.91$, $P < 0.001$). The errors between the MRI measurements and optical image analysis in patients with fatty deposits of ≤33% and more than 33% were 3.2 ± 2.5 and 3.9 ± 1.0%, respectively. As shown in Figs. 7 and 8, such a favorable correlation was maintained even in patients with significant fibrosis (stage 2–4, $n = 6$) or active lobular inflammation (score 2 and 3, $n = 13$) ($r = 0.93$ and $r = 0.94$, $P < 0.001$, respectively).

NAFLD, especially NASH, is reported to be sometimes associated with increased iron deposition in the liver, and severe iron deposition may affect the MR SI. Liver iron deposition was detected in three patients, and all the patients met the criteria for grade 1. The errors between the MRI measurements and the optical image analysis in patients without and with iron deposits were 3.3 ± 2.5 and 2.4 ± 2.1%, respectively.

## Discussion

In the present study, hepatic fat content, estimated by MRI on the basis of MR theory, was significantly correlated with hepatic fat content calculated by histological evaluation. Furthermore, even in patients with mild steatosis or significant fibrosis, quantification using this method tended to show a good correlation. These results demonstrate that the combination of a detailed MRI calibration using a water–oil phantom and double-echo FLASH sequence has accuracy comparable to that of estimates from liver histology in quantifying hepatic fat content. As far as we know, this is the first prospective study to validate the accuracy and utility of this convenient MR method for quantifying liver fat content.

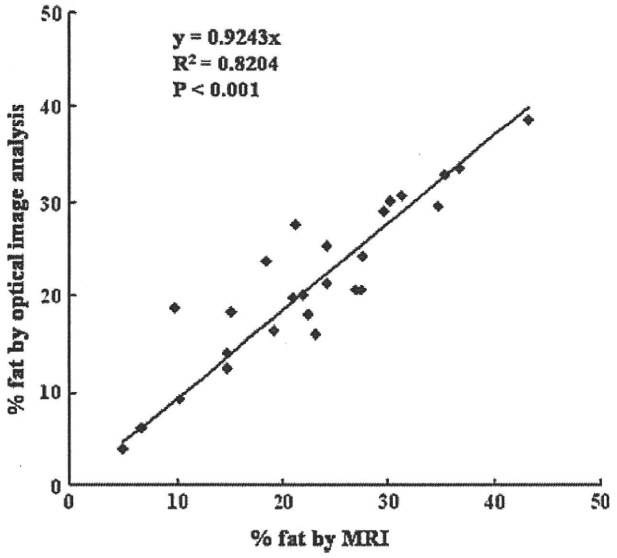


**Fig. 6** Relationship between MRI measurements of liver fat content in nonalcoholic fatty liver disease (NAFLD) patients and estimates made by optical image analysis of liver biopsy specimens ($n = 26$)

MR approaches for the quantification of hepatic fat content are divided into two categories: MRI and MR spectroscopy (MRS). Investigating the chemical shift by the application of spin-echo pulse sequences, the so-called Dixon method [12], has already shown significant correlations for the quantitative assessment of hepatic fat content. However, this MR technique was limited by an increased scanning time, which had to rely on the patient's ability to hold their breath. MRS has also been validated as a reliable test for quantifying liver fat [29, 30], but it relies on a single measurement from a predetermined ROI. Thus, it does not provide an assessment of the whole liver, or the retrospective selection of an ROI.

We selected a chemical shift MRI technique, i.e., the double-echo FLASH technique, in this study, because this technique has the following advantages: (1) it ensures that both IP and OP images are obtained from the same anatomic position, regardless of the patient's ability to hold their breath, so that it eliminates the problem of slice misintegration that can occur when two acquisitions are

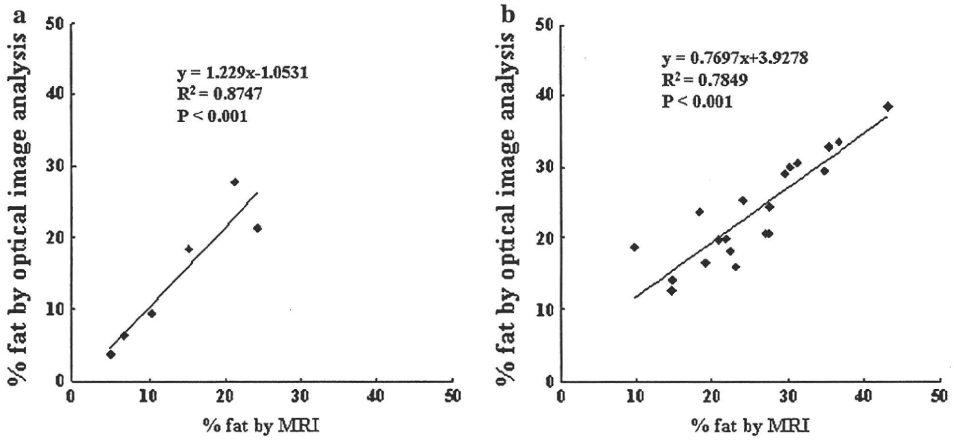


**Fig. 7** Relationship between MRI measurements of liver fat content and estimates made by optical image analysis of liver biopsy specimens in patients with **a** significant fibrosis (stage 2–4, $n = 6$) or **b** not (stage 0 and 1A, $n = 20$)

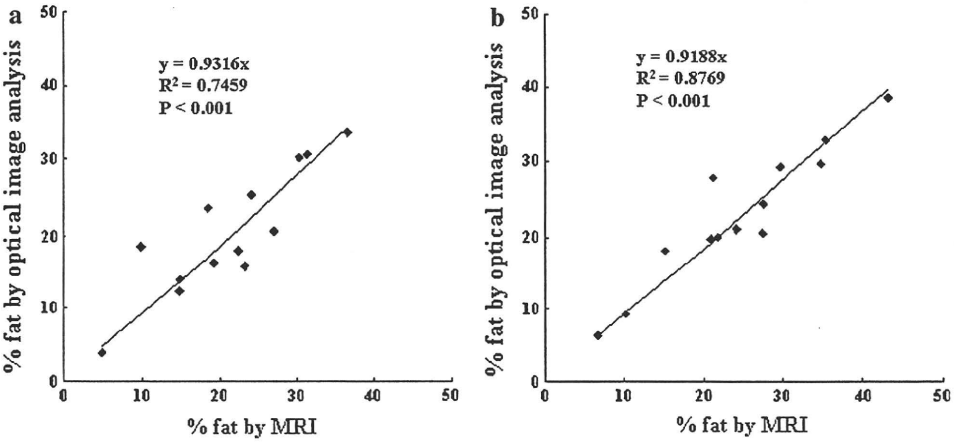


**Fig. 8** Relationship between MRI measurements of liver fat content and estimates made by optical image analysis of liver biopsy specimens in patients with lobular inflammation score **a** 0 and 1 ($n = 13$), **b** score 2 and 3 ($n = 13$)

performed, (2) all of the parameters except the TE are similar between IP and OP, and therefore the differences in MR SI between the two images are based only on parallel, respectively opposed water and fat protons. The 2-point and 3-point Dixon method could be compared with double-echo FLASH MRI, but the latter method is superior to the former in that the 3-point Dixon method was less affected by iron than the 2-point one [31, 32]. Though the 3-point Dixon method has not become widely used, the fat-quantification method using phantom-calibration in the present study is directly applicable to it.

The remarkable advantage of our method is that there is no need for special hardware and software. Therefore, at any institution having a 1.5-T MRI scanner, the quantification of hepatic steatosis based on this method can be performed, although the preparatory step of the collection of phantom data for each MRI scanner is needed for the evaluation of patient data. This preparation step appears to be difficult, but is actually simple and easy when a skilled MRI technician cooperates with the radiologist, because the phantom study can be performed without any special materials or software. Admittedly, it takes some time to prepare this step. However, this preparation is the only indispensable step for accurate quantification. Recent studies have demonstrated that a technique using selective saturation with a 3.0-T MRI scanner quantified liver fat content relatively well [21, 33], but 3.0-T MRI scanners are not commonly available at present.

Many previous studies using MRI were not calibrated through comparison with a phantom, and less reproducibility was obtained than with the technique described here [19–23]. In contrast with these previous studies, we compared MRI findings with optical image analysis data using software and found that measurements from the two modalities were linearly related and highly correlated. In most previous studies performed to compare MRI measurements with actual hepatic fat content, histopathological evaluation was limited to subjective semiquantitative grading by pathologists. Therefore, if the grade of fat deposition after therapy was the same as before, this conventional method could not reveal small changes in fat deposition. This problem, however, could be resolved by our methods.

In our MRI method, there is a possibility to underestimate the degree of fat deposition in patients with severe steatosis. Because the OP images accurately reflect the differences in water and fat signals, it is impossible to identify whether fat or water is the dominant signal. For example, the SI on OP images in the condition with "water:fat = 40:60" and that in the condition with "water:fat = 60:40" are equal. Therefore, a combination with other methods (e.g., MRS) or other imaging modalities (e.g., US, CT) is needed to evaluate hepatic fat content accurately if severe steatosis is suspected.

Gradient-echo sequences have high sensitivity to local magnetic field inhomogeneity caused by iron deposition, and iron deposition in the liver could mask the presence of fat on OP MR imaging. Westphalen et al. [34] showed that MRI evaluation was significantly correlated with the histopathologically determined liver fat percentage in patients without iron deposition, while no such correlation was found in patients with iron deposition. It is necessary to consider the influence of iron concentration on the application of our method to liver fat evaluation depending on objective disease (e.g., hepatitis C). The 3-point Dixon method has the advantage that there is no need to take into account the influence of iron deposits, but this sequence is inferior to our method with respect to general versatility because this sequence is cannot be performed without using special software at the present time.

To follow the clinical course and therapeutic response in NAFLD/NASH patients, appropriate means to quantitatively evaluate hepatic fat content are needed.Quantification of hepatic fat content using MRI in the present study was comparable to that based on histological evaluation even in humans with mild fatty deposition in the liver. Additionally, the present method is noninvasive and can be performed easily and repeatedly. Therefore it may be applicable not only for routine follow-up and evaluation of therapeutic response for NAFLD/NASH patients, but also for annual health checkups in healthy individuals and preoperative examination of candidate donors for living-related liver transplantation.

Clinically, accurate and noninvasive methods to distinguish NASH from NAFLD are desired. Recently, Iijima et al. [35] reported that contrast-enhanced US (using Levovist, Schering, Berlin, Germany) was a useful screening examination for NASH. In their study, the differential finding between NASH and NAFLD in delayed-phase contrast enhancement was attributed to a change in the sinusoidal endothelial system. If a new MRI contrast agent is developed that reflects pathological changes such as the perisinusoidal fibrosis seen in NASH, both the accurate quantification of hepatic fat content and the diagnosis of NASH might be obtained with a single MRI examination.

In conclusion, the double-echo FLASH technique on a 1.5-T MRI scanner provides a simple, accurate, and noninvasive means to quantify liver fat content. Although this was a prospective validation study, the number of patients enrolled was small and mild steatosis was the predominant condition. Further studies are needed to confirm the clinical usefulness of this convenient method.

## References


1. Falck-Ytter Y, Younossi ZM, Marchesini G, McCullough AJ. Clinical features and natural history of nonalcoholic steatosis syndromes. Semin Liver Dis. 2001;21:17–26.
2. Clark JM, Brancati FL, Diehl AM. Nonalcoholic fatty liver disease. Gastroenterology. 2002;122:1649–57.
3. Sanyal AJ. AGA technical review on nonalcoholic fatty liver disease. Gastroenterology. 2002;123:1705–25.
4. Clark JM, Brancati FL, Diehl AM. The prevalence and etiology of elevated aminotransferase levels in the United States. Am J Gastroenterol. 2003;98:960–7.
5. Kleiner DE, Brunt EM, Van Natta M, Behling C, Contos MJ, Cummings OW, et al. Design and validation of a histological scoring system for nonalcoholic fatty liver disease. Hepatology. 2005;41:1313–21.
6. Nonomura A, Enomoto Y, Takeda M, Tamura T, Kasai T, Yoshikawa T, et al. Clinical and pathological features of non-alcoholic steatohepatitis. Hepatol Res. 2005;33:116–21.
7. Matteoni CA, Younossi ZM, Gramlich T, Boparai N, Liu YC, McCullough AJ. Nonalcoholic fatty liver disease: a spectrum of clinical and pathological severity. Gastroenterology. 1999;116:1413–9.
8. Brunt EM, Janney CG, Di Bisceglie AM, Neuschwander-Tetri BA, Bacon BR. Nonalcoholic steatohepatitis: a proposal for grading and staging the histological lesions. Am J Gastroenterol. 1999;94:2467–74.
9. Siegelman ES, Rosen MA. Imaging of hepatic steatosis. Semin Liver Dis. 2001;21:71–80.
10. Ricci C, Longo R, Gioulis E, Bosco M, Pollesello P, Masutti F, et al. Noninvasive in vivo quantitative assessment of fat content in human liver. J Hepatol. 1997;27:108–13.
11. Saadeh S, Younossi ZM, Remer EM, Gramlich T, Ong JP, Hurley M, et al. The utility of radiological imaging in nonalcoholic fatty liver disease. Gastroenterology. 2002;123:745–50.
12. Dixon WT. Simple proton spectroscopic imaging. Radiology. 1984;153:189–94.
13. Lee JK, Dixon WT, Ling D, Levitt RG, Murphy WA. Fatty infiltration of the liver: demonstration by proton spectroscopic imaging. Radiology. 1984;153:195–201.
14. Fishbein MH, Gardner KG, Potter CJ, Schmalbrock P, Smith MA. Introduction of fast MR imaging in the assessment of hepatic steatosis. Magn Reson Imaging. 1997;15:287–93.
15. Delfaut EM, Beltran J, Johnson G, Rousseau J, Marchandise X, Cotten A. Fat suppression in MR imaging: techniques and pitfalls. Radiographics. 1999;19:373–82.
16. Mitchell DG, Kim I, Chang TS, Vinitski S, Consigny PM, Saponaro SA, et al. Chemical shift phase-difference and suppression magnetic resonance imaging techniques in animals, phantoms, and humans. Invest Radiol. 1991;26:1041–52.
17. Levenson H, Greensite F, Hoefs J, Friloux L, Applegate G, Silva E, et al. Fatty infiltration of the liver: quantification with phase contrast MR imaging at 1.5 T vs biopsy. AJR Am J Roentgenol. 1991;156:307–12.
18. Namimoto T, Yamashita Y, Mitsuzaki K, Nakayama Y, Makita O, Kadota M, et al. Adrenal masses: quantification of fat content with double-echo chemical shift in-phase and opposed-phase FLASH MR images for differentiation of adrenal adenomas. Radiology. 2001;218:642–6.
19. Rinella ME, McCarthy R, Thakrar K, Finn JP, Rao SM, Koffron AJ, et al. Dual-echo, chemical shift gradient-echo magnetic resonance imaging to quantify hepatic steatosis: implications for living liver donation. Liver Transpl. 2003;9:851–6.
20. Pilleul F, Chave G, Dumortier J, Scoazec JY, Valette PJ. Fatty infiltration of the liver: detection and grading using dual T1 gradient echo sequences on clinical MR system. Gastroenterol Clin Biol. 2005;29:1143–7.
21. Schuchmann S, Weigel C, Albrecht L, Kirsch M, Lemke A, Lorenz G, et al. Non-invasive quantification of hepatic fat fraction by fast 1.0, 1.5, 3.0 T MR imaging. Eur J Radiol. 2007;62:416–22.
22. Hussain HK, Chenevert TL, Londy FJ, Gulani V, Swanson SD, McKenna B, et al. Hepatic fat fraction: MR imaging for quantitative measurement and display—early experience. Radiology. 2005;237:1048–55.
23. Kim SH, Lee JM, Han JK, Lee JY, Lee KH, Han CJ, et al. Hepatic macrosteatosis: predicting appropriateness of liver donation by using MR imaging—correlation with histopathologic findings. Radiology. 2006;240:116–29.
24. The Examination Committee of Criteria for 'Obesity Diseases' in Japan, Japan Society for the Study of Obesity. New criteria for 'Obesity Disease' in Japan. Circ J. 2002;66:987–92.
25. Tanaka N, Ichijo T, Okiyama W, Mutou H, Misawa N, Matsumoto A, et al. Laparoscopic findings in patients with non-alcoholic steatohepatitis. Liver Int. 2006;26:32–8.
26. Tanaka N, Tanaka E, Sheena Y, Komatsu M, Okiyama W, Misawa N, et al. Useful parameters for distinguishing nonalcoholic steatohepatitis with mild steatosis from cryptogenic chronic hepatitis in the Japanese population. Liver Int. 2006;26:956–63.
27. Tanaka N, Sano K, Horiuchi A, Tanaka E, Kiyosawa K, Aoyama T. Highly-purified eicosapentaenoic acid treatment improves nonalcoholic steatohepatitis. J Clin Gastroenterol. 2008;42:413–8.
28. Searle JW, Kerr JFR, Halliday JW, Powell LW. Iron storage disease. In: MacSween RNM, Anthony PP, Scheuer PJ, editors. Pathology of the liver. 2nd ed. Edinburgh: Churchill Livingstone; 1987.
29. Szczepaniak LS, Babcock EE, Schick FD, Garg A, Dobbins RL, Burns T, et al. Measurement of intracellular triglyceride stores by H spectroscopy and validation in vivo. Am J Physiol. 1999;276:E977–89.
30. Longo R, Pllesello P, Ricci C, Masutti F, Kvam BJ, Bercich L, et al. Proton MR spectroscopy in quantitative in vivo determination of fat content in human steatosis. J Magn Reson Imaging. 1995;5:281–5.
31. Lodes CC, Felmlee JP, Ehman RL, Sehgal CM, Greenleaf JF, Glover GH, et al. Proton MR chemical shift imaging using double and triple phase contrast acquisition methods. J Comput Assist Tomogr. 1989;13:855–61.
32. Szumowski J, Coshow WR, Li F, Quinn SF. Phase unwrapping in the three-point Dixon method for fat suppression MR imaging. Radiology. 1994;192:555–61.
33. Cotler SJ, Guzman G, Layden-Almer J, Mazzone T, Layden TJ, Zhou XJ. Measurement of liver fat content using selective saturation at 3.0 T. J Magn Reson Imaging. 2007;25:743–8.
34. Westphalen AC, Qayyum A, Yeh BM, Merriman RB, Lee JA, Lamba A, et al. Liver fat: effect of hepatic iron deposit on evaluation with opposed-phase MR imaging. Radiology. 2007; 242:450–5.
35. Iijima H, Moriyasu F, Tsuchiya K, Suzuki S, Yoshida M, Shimizu M, et al. Decrease in accumulation of ultrasound contrast microbubbles in non-alcoholic steatohepatitis. Hepatol Res. 2007;37:722–30.

J Korean Med Sci 2010; 25: 476-80

ISSN 1011-8934
DOI: 10.3346/jkms.2010.25.3.476

# A Case of Granulocyte-Colony Stimulating Factor-Producing Hepatocellular Carcinoma Confirmed by Immunohistochemistry

Granulocyte-colony stimulating factor (G-CSF) is a naturally occurring glycoprotein that stimulates the proliferation and maturation of precursor cells in the bone marrow into fully differentiated neutrophils. Several reports of G-CSF-producing malignant tumors have been published, but scarcely any in the hepatobiliary system, such as in hepatocellular carcinoma (HCC). Here, we encountered a 69-yr-old man with a hepatic tumor who had received right hepatic resection. He showed leukocytosis of 25,450/$\mu$L along with elevated serum G-CSF. Histological examination of surgical samples demonstrated immunohistochemical staining for G-CSF, but not for G-CSF receptor. The patient survived without recurrence for four years, but ultimately passed away with multiple bone metastases. In light of the above, clinicians may consider G-CSF-producing HCC when encountering patients with leukocytosis and a hepatic tumor. More cases are needed to clarify the clinical picture of G-CSF-producing HCC.

Key Words : *G-CSF-producing Tumor; Carcinoma, Hepatocellular; Immunohistochemistry*



**Satoru Joshita[1,2], Koh Nakazawa[3], Shoichiro Koike[4], Atsushi Kamijo[1,2], Kiyoshi Matsubayashi[1], Hideharu Miyabayashi[1], Kiyoshi Furuta[1], Kiyoshi Kitano[1], Kaname Yoshizawa[2], and Eiji Tanaka[2]**

Department of Internal Medicine[1], Matsumoto Medical Center, Matsumoto; Department of Internal Medicine[2], Division of Gastroenterology and Hepatology, Shinshu University School of Medicine, Matsumoto; Departments of Laboratory Medicine[3] and Surgery[4], Matsumoto Medical Center, Matsumoto, Japan

Received : 21 November 2008
Accepted : 4 March 2009

**Address for Correspondence**
Satoru Joshita, M.D.
Department of Internal Medicine, Division of Gastroenterology and Hepatology, Shinshu University School of Medicine, 3-1-1 Asahi, Matsumoto 390-8621, Japan
Tel : +81-263-37-2634, Fax : +81-263-32-9412
E-mail : joshita@shinshu-u.ac.jp

## INTRODUCTION

The concept of colony stimulating factor (CSF) as a hematopoietic induction, differentiation, and growth factor was first discussed in 1966 (1). A case of malignancy was later reported with increased CSF activation in serum and urine in 1974 (2). Afterwards, it was demonstrated for the first time that CSF was directly produced in a lung cancer tissue specimen in 1977 (3).

Granulocyte-colony stimulating factor (G-CSF) is recognized as a naturally occurring glycoprotein that stimulates the proliferation and maturation of precursor cells in the bone marrow into fully differentiated neutrophils (4). Although several accounts of G-CSF-producing malignant tumors in lung cancer exist, few have been observed in the digestive system. Notably, there have been scarcely any cases found in primary liver cancer, such as hepatocellular carcinoma (HCC). Here, we present a rare case of G-CSF-producing HCC that was confirmed by immunohistochemistry.

## CASE REPORT

A 69-yr-old man was admitted to our hospital in July 1999 suffering from fever, general fatigue, weight loss, and right upper abdominal pain.

On examination, the patient was 157 cm tall and weighed 43 kg. His temperature was 36.2°C. He showed no signs of alcohol addiction and had no indications of co-morbidities, such as diabetes mellitus or dyslipidemia. His family medical history was clear of any hepatic disorders. He had no signs of anemia or jaundice in conjunctiva and presented with no abdominal masses or hepatosplenomegaly, but did complain of tenderness on the right side hypochondrium. Neurological and chest examinations revealed no abnormal findings.

Laboratory tests showed a white blood cell count of 25,450/$\mu$L with 90% neutrophils, a red blood cell count of $367 \times 10^4$/$\mu$L, and a platelet count of $35.2 \times 10^4$/$\mu$L. His hemoglobin value was 10.1 g/dL and hematocrit was 31.2%. Blood chemistry showed aspartate aminotransferase of 57 U/L, alanine aminotransferase of 36 U/L, alkaline phosphatase of 949 U/L (normal range: 115 to 359 U/L), gamma-glutamyl transpeptidase of 313 U/L, cholinesterase of 44 U/L, total protein of 6.7 g/dL, and total albumin of 2.7 g/dL. C-reactive protein (CRP) was found to be 13.1 mg/dL in serological studies. The serum level of AFP was 2.0 ng/mL, the level of protein induced by vitamin K absence or antagonist II (PIVKA II)

was 43 mAU/mL, the level of CEA was 9.9 ng/mL(normal value: less than 5.0 ng/mL), and the level of CA19-9 was 6.0 U/mL. Tests for hepatitis B virus surface antigen (HBsAg), hepatitis B core antibody (HBcAb), and hepatitis C virus antibody were all negative. Elevations in serum G-CSF and interleukin-6 (IL-6) were seen at 62 pg/mL (normal value: less than 18.1 pg/mL) and 26.7 pg/mL (normal value: less than 4.0 pg/mL), respectively. Bone marrow aspiration and a biopsy specimen revealed hypercellularity of mature neutrophils with normal erythropoiesis and megakaryopoiesis.

A hypoechoic tumor 5 cm in diameter was detected by ultrasonography between the anterior inferior segment (S5) and anterior superior segment (S8) of the liver. The tumor presented as a slightly low density area in pre-contrasted computed tomography (CT). It was enhanced in early phase contrast enhanced CT and accompanied with diffuse enhancement in the surrounding area, and finally washed out in the late phase with delayed hyper-enhancement in the surrounding area (Fig. 1). Magnetic resonance imaging (MRI) showed low and high intensity nodules in T1 and T2 weighted imaging with fat suppression, respectively. Angiographic examination showed that the tumor had hypervascularity. We clinically diagnosed the hepatic tumor to be common HCC according to these findings and the surrounding area to be secondary inflammatory change associated with the tumor.

We initially considered the possibility of co-infection since the patient had fever, extreme leukocytosis, and high serum levels of CRP. We intravenously administered 2 g/day sulbactam/cefoperazone and 2,400 mg/day clindamycin for 10 days, and then changed treatment to 1 g/day meropenem and 2,400 mg/day clindamycin for 9 days. No effects were seen, nor could we detect any infective foci in other organ sites by radiography or CT. Blood cultures were also tested several times after admission but were all negative for bacteria and fungus. CT images of the tumor before and after antibiotic administration did not differ. Based on the above, we concluded that the patient had no co-infections and diagnosed him as having a paraneoplastic syndrome.

The patient received right hepatic resection in September later that year. His blood leukocyte counts decreased to normal range, and serum G-CSF and IL-6 deceased to 12 pg/mL and 5.9 pg/mL, respectively. An encapsulated gray-white nodule with foci of necrosis was seen by cut surface of the resected liver (Fig. 2A). Resected specimens of tumor histologically revealed that the tumor was a moderately differentiated hepatocellular carcinoma (Fig. 2B). A specimen of liver parenchyma adjacent to the tumor, which was diffusely enhanced by contrast enhanced CT, showed marked infiltration with neutrophils within the widened sinusoid that represented congestion (Fig. 2C). The tumor showed positive staining for hepatocyte paraffin 1 (Hep par 1) and G-CSF (Anti-G-CSF [Ab-1], mouse monoclonal antibody, Calbiochem, Darmstadt, Germany) in the cytoplasm, but was negative for G-CSF receptor (G-CSF receptor antibody [S-1284], mouse monoclonal antibody, Abcam, Cambridge, UK) (Fig. 2D-F). We thus diagnosed this tumor as a G-CSF-producing hepatocellular carcinoma.

The patient had regular follow-ups for about four years without any recurrence. He experienced rib pain in 2003 and was diagnosed as having multiple bone metastases by several imaging examinations. He was admitted to our hospital again for palliative care, and succumbed to his illness one month later. His serum G-CSF at the time of death was 18 pg/mL and within normal range.

## DISCUSSION

All cases of G-CSF-producing HCC reported in English literature are listed in Table 1 (5, 6). As G-CSF-producing

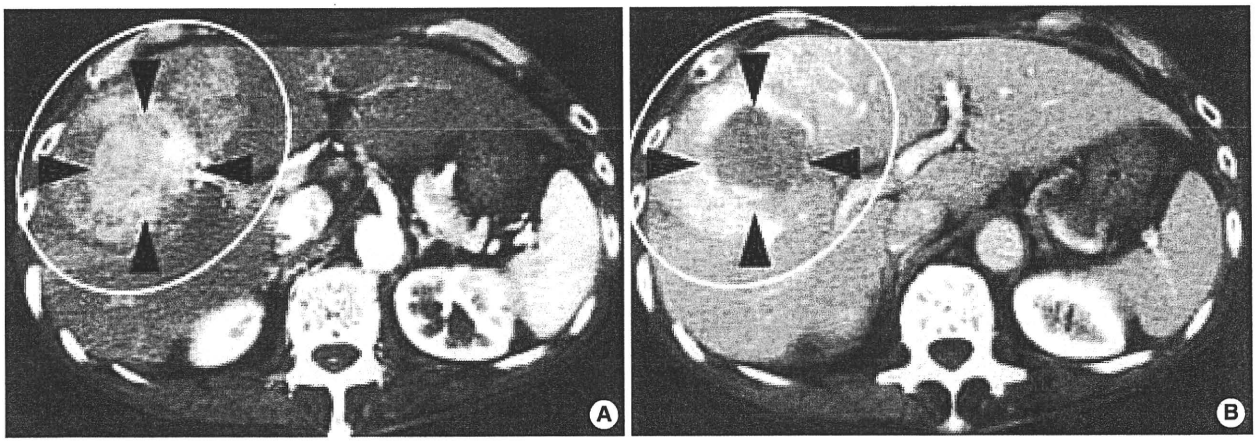


Fig. 1. Computed tomography findings. (A) The tumor measuring 5 cm in diameter between the anterior inferior segment (S5) and the anterior superior segment (S8) of the liver showed hyper-enhancement (black arrow heads) in the early phase of dynamic enhanced CT accompanied with diffuse enhancement in the surrounding area (white circle). (B) It showed complete washout (black arrow heads) in the late phase with delayed hyper-enhancement in the surrounding area (white circle).

HCC is extremely rare, only two cases have been documented until now. Here, we present the third such case, along with immunohistochemical proof of G-CSF expression.

The following findings are indicative of G-CSF producing tumors: elevation of serum G-CSF and an increased leukocyte count, transient decreases in G-CSF and leukocyte count to normal ranges after tumor resection, a simultaneous increase in G-CSF and neutrophil count with tumor recurrence, and an elevation in G-CSF expression levels in resected specimens on the basis of immunohistochemical staining or real-time reverse transcriptase polymerase chain reaction. One direct way to prove G-CSF production on the tumor cells is by immunohistochemical techniques (7). In this case, we could clearly demonstrate that the hepatic tumor produced G-CSF by immunohistochemical analysis of specimens taken during his operation (Fig. 2E). Extreme leukocytosis and signif-

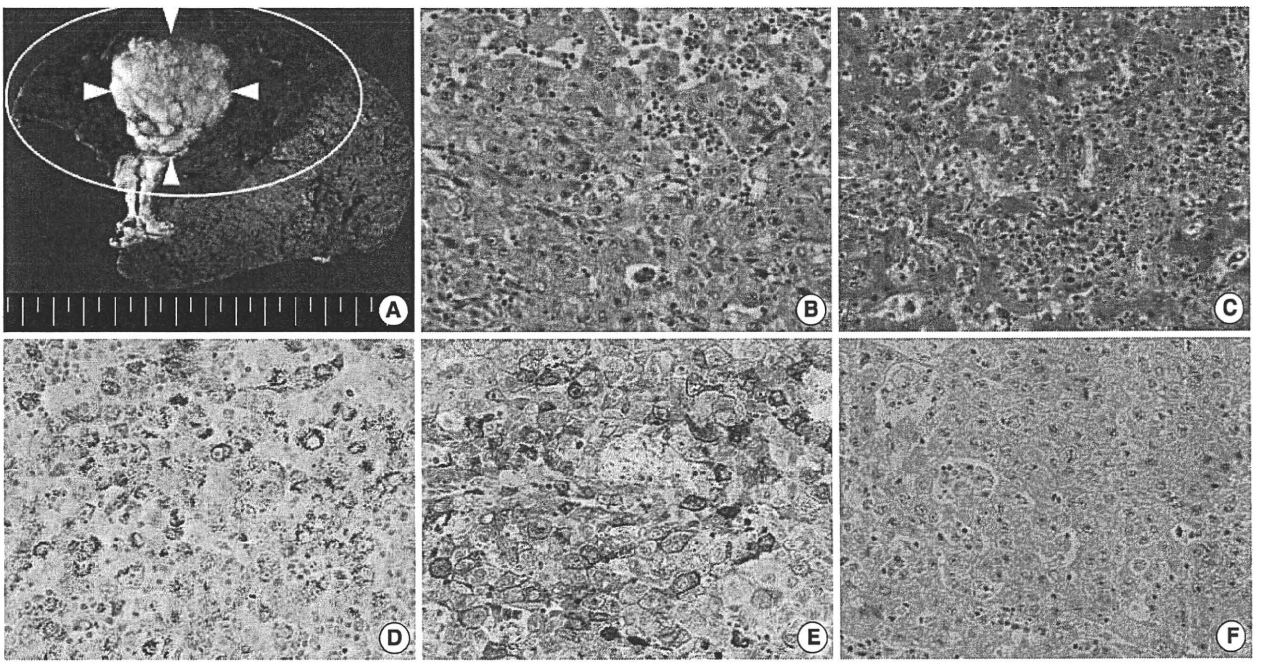


Fig. 2. Gross and microscopic findings of the tumor. (A) Cut surface of the resected liver showed an encapsulated gray-white nodule (white arrow heads) with foci of necrosis. The area adjacent to the tumor (white circle) revealed prominent congestion. Non-neoplastic liver parenchyma was not cirrhotic. (B) Microscopic findings showed atypical cells lying in sheets with marked infiltration of neutrophils and lymphocytes, which were diagnosed as a moderately differentiated hepatocellular carcinoma (H&E, ×20 magnification of the objective lens). (C) Liver parenchyma adjacent to the tumor, diffusely enhanced by contrast enhanced CT, showed prominent congestion and marked infiltration with neutrophils within the widened sinusoid (H&E, ×20 magnification of the objective lens). The other parts of liver did not present findings of chronic hepatitis or cirrhosis (not shown). (D) The tumor lesion was stained with hepatocyte paraffin 1 (Hep par 1) (×20 magnification of the objective lens). (E) Immunohistochemical examination also showed positive staining for granulocyte-colony stimulating factor (G-CSF) in the cytoplasm of atypical cells (×20 magnification of the objective lens). (F) Immunohistochemical examination showed negative staining for G-CSF receptors in the tumor cells (×20 magnification of the objective lens).

Table 1. Clinical findings of granulocyte-colony stimulating factor-producing hepatocellular carcinoma in English literature

| Case | Age | Gender | HCV | WBC /μL | G-CSF pg/mL (<18.1) | IL-6 pg/mL (<4.0) | Pathology | Treatment | Prognosis* |
|---|---|---|---|---|---|---|---|---|---|
| 1 (5) | 67 | M | SVR | 27,000 | 521 | NT | Poorly differentiated hepatocellular carcinoma | TAE+Chemotherapy | 5 months |
| 2 (6) | 66 | M | - | 16,600 | 178 | 26.4 | Poorly differentiated hepatocellular carcinoma | Radical surgery+TAE | 4 months |
| Our case | 69 | M | - | 25,450 | 62 | 26.7 | Moderately differentiated hepatocellular carcinoma | Radical surgery | 4 yr |

*Prognosis began at diagnosis.
HCV, hepatitis C virus; WBC, white blood cell; G-CSF, granulocyte-colony stimulating factor; IL-6, interleukin-6; M, male; SVR, sustained virological response; NT, not tested; TAE, transcatheter arterial embolization.